

Oligonucleotide-based biosensors for in vitro diagnostics and environmental hazard detection

Il Young Jung¹ · Eun Hee Lee¹ · Ah Young Suh¹ · Seung Jin Lee¹ · Hyukjin Lee¹

Received: 21 August 2015 / Revised: 19 October 2015 / Accepted: 23 November 2015 / Published online: 18 January 2016
© Springer-Verlag Berlin Heidelberg 2016

Abstract Oligonucleotide-based biosensors have drawn much attention because of their broad applications in in vitro diagnostics and environmental hazard detection. They are particularly of interest to many researchers because of their high specificity as well as excellent sensitivity. Recently, oligonucleotide-based biosensors have been used to achieve not only genetic detection of targets but also the detection of small molecules, peptides, and proteins. This has further broadened the applications of these sensors in the medical and health care industry. In this review, we highlight various examples of oligonucleotide-based biosensors for the detection of diseases, drugs, and environmentally hazardous chemicals. Each example is provided with detailed schematics of the detection mechanism in addition to the supporting experimental results. Furthermore, future perspectives and new challenges in oligonucleotide-based biosensors are discussed.

Keywords Biosensors · Oligonucleotide · In vitro diagnosis · Environmental hazard detection

Abbreviations

A β Amyloid β
ACNG Aptamer-coated nanogold

AD	Alzheimer's disease
ADDL	Amyloid β derived diffusible ligand
AuNP	Gold nanoparticle
Au@PtNP	Nanoparticle consisting of a gold core and a platinum shell
BPA	Bisphenol A
cDNA	Complementary DNA
CEA	Carcinoembryonic antigen
CSF	Cerebrospinal fluid
EDC	Endocrine-disrupting compound
FRET	Fluorescence resonance energy transfer
G4	G-quadruplex
HBV	Hepatitis B virus
HRCA	Hyperbranched rolling circle amplification
HRP	Horseradish peroxidase
LSPR	Localized surface plasmon resonance
MB-AuNPs	Gold nanoparticles with magnetic microbeads inside
mHCR	Multibranched hybridization chain reaction
MWCNT	Multiwalled carbon nanotube
NPG	Nanoporous gold
OTA	Ochratoxin A
PCR	Polymerase chain reaction
PDGF	Platelet-derived growth factor
PrP ^c	Cellular prion protein
QCM	Quartz crystal microbalance
QD	Quantum dot
RCA	Rolling circle amplification
RT-PCR	Reverse transcription polymerase chain reaction
SELEX	Systemic evolution of ligands by exponential enrichment
SERRS	Surface-enhanced resonance Raman scattering
ssDNA	Single-stranded DNA
TAMRA	Tetramethylrhodamine
THMS	Triple-helix molecular switch

ABC Highlights: authored by *Rising Stars and Top Experts*.

Il Young Jung, Eun Hee Lee, and Ah Young Suh contributed equally to this work.

✉ Hyukjin Lee
hyukjin@ewha.ac.kr

¹ College of Pharmacy, Graduate School of Pharmaceutical Sciences, Ewha Womans University, Seoul 03760, Republic of Korea

Introduction

Biosensors are quantitative analytical tools which contain biological materials and physicochemical signal transducers. Biological materials such as DNA/RNA pathogens, proteins, and chemicals can specifically recognize and relate the concentration of the target analyte to a measurable biological response. Signal transducers then convert the response to various reporting signals. If the analyte binds to the receptor, changes in pH, heat, light, mass, and so forth can occur [1]. This change is translated to a reporting signal, and various recognition elements can be used in biosensors, such as small chemicals, enzymes, proteins, antibodies, DNA, organelles, microbial cells, plants, and animal tissues.

With increasing demand for biosensors in drug development and medical diagnosis, various biosensors have been developed for particular applications [2]. The value of the global biosensor market was USD 12.46 billion in 2013 and is expected to grow by 8.1 % per year from 2014 to 2020 [3]. Examples of commonly used biosensors in real life include the pregnancy test, which detects human chorionic gonadotropin in urine, glucose monitoring devices for patients with diabetes, and the tuberculosis detection test for identification of the infectious disease in a few minutes. Besides these, applications of biosensors are not limited to the health care industry and are also applicable to food analysis, crime detection, and environmental field monitoring.

Among various biosensors, oligonucleotide-based biosensors are of much interest to many researchers because they can serve the dual role of detection and amplification of target analytes by simple base-pair hybridization and amplification by polymerization. In contrast to traditional methods such as antibody-based biosensors, oligonucleotide-based biosensors use the base pairings of oligonucleotides. Hybridization between nucleic acids is stable and highly specific. Also oligonucleotide-based biosensors use an aptamer, which is a short oligonucleotide showing strong binding affinity toward target molecules. An aptamer is useful tool to detect proteins, heavy metals, and other chemicals that do not have a sequence-specific hybridization property. However, an aptamer shows a quite different binding mechanism as compared with the sequence specific hybridization of DNA or RNA. The binding mechanism between aptamers and target molecules is variable according to the systems. The common forces between them are electrostatic and hydrophobic interactions. Many aptamers selectively bind to the target molecules by their designed structures in addition to their sequences. Therefore, oligonucleotide-based biosensors show good flexibility of oligonucleotide design in various applications. Because of their high specificity, stability, and variability for the base-pairing hybridization for detection and diagnosis, oligonucleotide-based biosensors are widely used in clinical diagnosis and genome mutation detection. However,

there are possible drawbacks of oligonucleotide-based biosensors. First, it is necessary to control the temperature during detection. This requires equipment such as a thermal cycler. Second, a fluorescent dye system is needed, requiring additional steps and equipment to detect fluorescence. For detection of target analytes, aptamers should be synthesized to detect specific target molecules. With systemic evolution of ligands by exponential enrichment (SELEX) technology, aptamers showing high binding affinity toward the target can be isolated. In SELEX, three cycles are constantly repeated: adsorption, recovery, and reamplification [4]. With the unique design of detection systems with various aptamers, the applicability of oligonucleotide-based biosensors has been further broadened. In this review, oligonucleotide-based biosensors are categorized according to their applications—that is, clinical diagnostics (inherited diseases, pathogenic infectious diseases), drug analysis, and environmental monitoring. Among numerous biosensors, we have focused on introducing oligonucleotide-based biosensors with extremely sensitive, rapid detection and relatively low cost of production.

Oligonucleotide-based biosensors for external diagnostic application

Biosensors for the detection of human diseases

An *in vitro* diagnostic is a tool for detecting disease through analysis of a body fluid such as blood, saliva, sputum, or tissue. In everyday life, *in vitro* diagnostics have been used for pregnancy tests or glucose-level tests. In addition, *in vitro* diagnostics can be used for detection various infectious diseases such as Ebola and Middle East respiratory syndrome and can be a monitoring tool for checking blood cholesterol level. The *in vitro* diagnostics market is growing by about 8 % per year. The US *in vitro* diagnostics market is largest in the world, accounting for almost 50 %. However, the Asian market is growing at the fastest rate [5].

Cancer

Circulating tumor cells have recently gained attention as predictive and prognostic biomarkers [6]. Highly sensitive detection of circulating tumor cells in the blood can allow early diagnosis of cancer and cancer metastasis [7–11]. However, it can be a challenging task to detect circulating tumor cells when their concentration in peripheral blood is very low; thus, the development of highly sensitive and specific detection methods is necessary [7–11]. Although some polymerase chain reaction (PCR)-based methods have already been applied to detect cancer cells, they are complicated, costly, and time-consuming and cannot be used to directly detect whole cancer cells because of a cell lysis step [7–10, 12–23].

Zuo et al. [24] designed DNA nanostructured biosensors based on multibranch hybridization chain reaction (mHCR) for multivalent capture and detection of cancer cells (Fig. 1a). In their study, epithelial cell adhesion molecule, which is expressed significantly on the surface of epithelial cancer cells, was used as a diagnostic biomarker for cancers. An initiator partially hybridized to the aptamer of epithelial cell adhesion molecule was added to the mixture of two sets of DNA hairpins (H1 and H2). Then, a long chain with multiple biotins and branched arms was generated by mHCR. When cancer cells are present, they conjugate with mHCR products. DNA tetrahedral probes immobilized on gold electrode surfaces can be used to capture cancer cells. Multivalent binding of cancer cells to the surface can be realized through multiple branched arms, which enhances the capturing efficiency. In addition, multiple avidin–horseradish peroxidase (HRP) conjugates attached to the biotin labels amplify the electrochemical signal, which increases the detection sensitivity. Electrochemical methods which use the electrocatalytic properties of HRP for H_2O_2 reduction were used for the rapid and sensitive detection of cancer cells captured on the surface of gold electrodes [24–29]. Electrocatalytic current was increased proportionally to the number of cancer cells. The electrochemical current with 1000 cancer cells was 450 nA in the method without amplification (Fig. 1b), but significantly increased to 8600 nA in the method with mHCR amplification (Fig. 1b) [24]. Furthermore, the detection limit of the method with HCR amplification was improved with as few as four cancer cells, whereas the conventional method required 24 or more cancer cells (Fig. 1b). These results suggest that the detection sensitivity is enhanced by the amplification of multiple HRPs attached to the mHCR products. In addition, almost no differences were observed between the number of cancer cells captured on the surface of the gold electrodes before and after the washing steps, suggesting there was improved capturing capacity and efficiency due to multivalent binding. Therefore, the synergetic effect of multivalent binding and signal amplification by the mHCR provides highly sensitive and specific detection of cancer cells.

Carcinoembryonic antigen (CEA) is another well-known tumor marker associated with many cancers (e.g. liver, colon, breast, and colorectal cancers) [30–33]. An aptamer with high binding affinity toward CEA was used for biosensing. Recently, a wide variety of biosensors for the detection of CEA have been developed with signal amplification techniques such as PCR and rolling circle amplification (RCA) [34]. Although RCA has the advantages of simplicity and efficiency, the sensitivity of RCA-based biosensors is generally lower than that of PCR [35].

Liang et al. [34] developed ultrasensitive hyperbranched RCA (HRCA)-based colorimetric biosensors for CEA as a way to overcome this limitation [36]. In the HRCA reaction, specific DNA fragments can be amplified exponentially

through replication of circularized probes under isothermal conditions [37, 38]. In the presence of the target protein (CEA), the CEA aptamer binds more specifically to CEA than to complementary DNA (cDNA), forming the CEA–aptamer complex [34]. Therefore, free cDNA is allowed to hybridize with the DNA template (padlock probe), which is subsequently ligated and circularized by *Escherichia coli* DNA ligase. After formation of circularized padlock probes, multiple single-stranded DNA (ssDNA) strands were produced by HRCA reaction. These strands are consequently adsorbed onto gold nanoparticles (AuNPs), and induce electrostatic repulsion between ssDNA-adsorbed AuNPs. Thus, when sodium citrate salt is added, the salt-induced AuNP aggregation can be prevented, and the solution remains red color. However, in the absence of the target protein (CEA), the CEA aptamer hybridizes with the short DNA primer (cDNA). Thus, there is no free cDNA to hybridize with the DNA template (padlock probe), and nothing can trigger the HRCA reaction. As a result, the amount of ssDNA strands is not enough to prevent salt-induced AuNP aggregation. When salt is added, the AuNPs aggregate, which leads to a color change of the solution. The absorption intensity ratio (A_{520}/A_{660}) is used for evaluation of the difference between the aggregation of AuNPs [36]. In the presence of CEA, the color of the solution is red and the absorption peak is observed around 520 nm. In the absence of CEA, however, there is a significant peak shift from 520 to 660 nm, accompanied by a chromatic transition from red to blue. In addition, a linear relationship between A_{520}/A_{660} and the logarithmic concentration of CEA was observed, which supports the proposed mechanism.

Neurodegenerative diseases

Prion proteins cause neurodegenerative diseases that affect humans or animals by disrupting the structure of the brain [39]. The mechanism of prion propagation is associated with the conversion of normal prion proteins (cellular prion protein, PrP^c) into pathogenic isoforms of prion proteins (scrapie-type prion protein) [40]. However, scrapie-type prion protein, the hallmark of prion diseases, can be observed only at the late stage, which makes early diagnosis of the diseases difficult [41]. In the last few decades, several biosensors have been developed that use the capacity of PrP^c to bind to nucleic acids (i.e., DNA and RNA) [42–46]. Xiao et al. [36] developed an aptamer-based fluorescence biosensor for the detection of PrP^c; the strategy involved is shown in Fig. 2a. There are three main components of the aptamer structure: (1) the core sequence located in the loop, (2) three guanine bases at the 3' terminal, and (3) tetramethylrhodamine (TAMRA) fluorophore modification at the 5' terminal. In the absence of target PrP^c, the guanine bases at the 3' terminal are close enough to TAMRA and quench the fluorescence of TAMRA via electron transfer. In the presence of the target PrP^c,

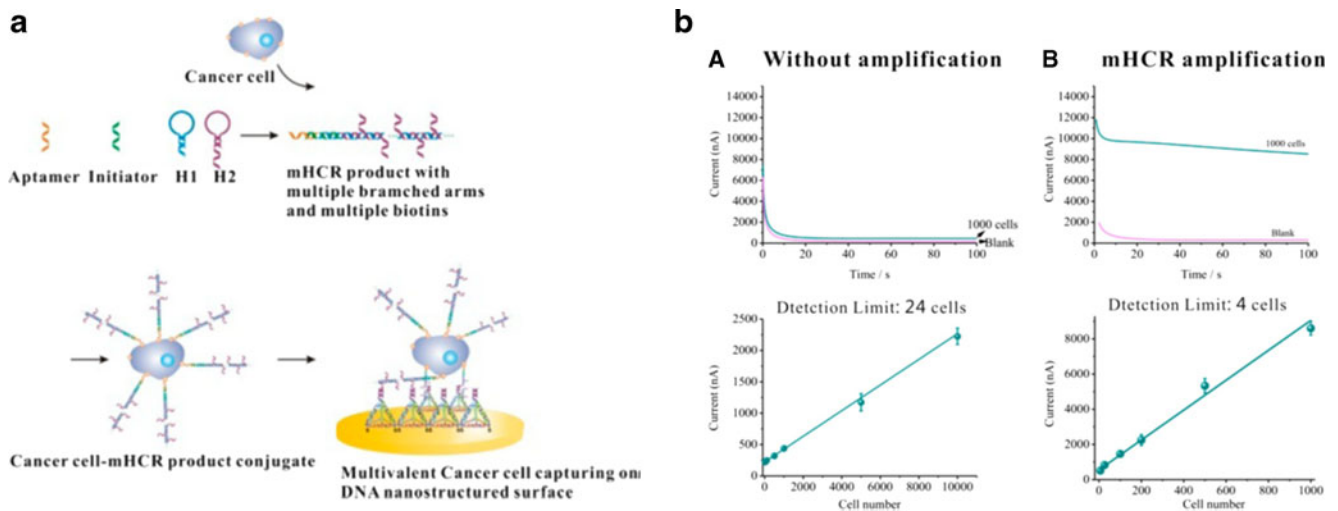


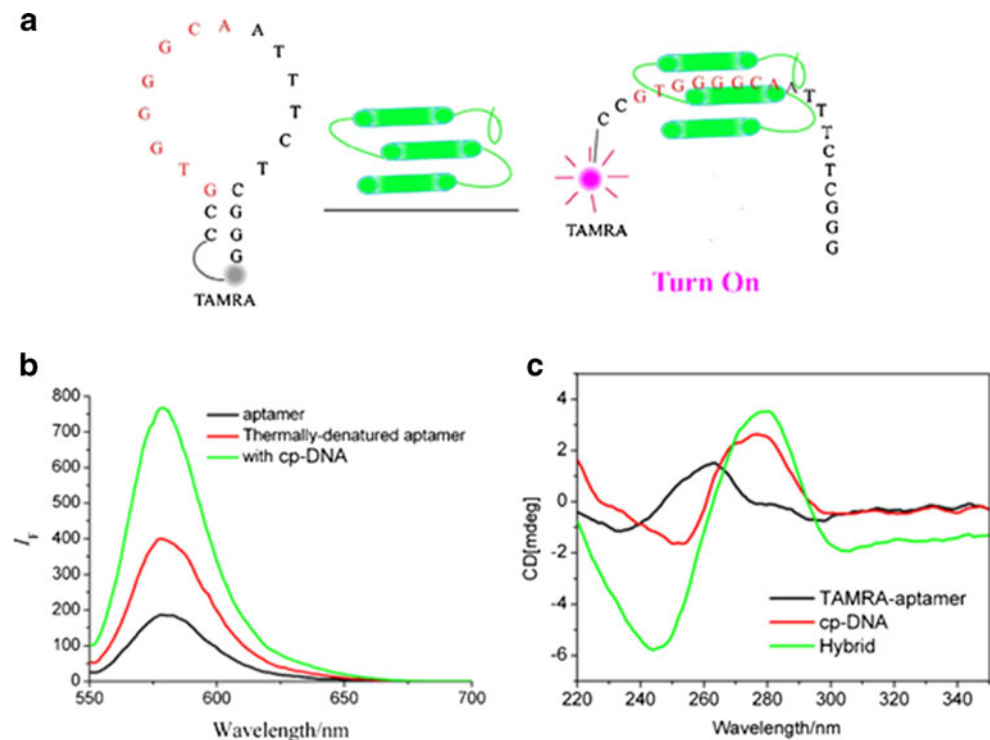
Fig. 1 **a** The long products with multiple biotin labels and multiple branched arms were synthesized by multibranching hybridization chain reaction (*mHCR*). The cancer cells conjugated with *mHCR* products can be attached to the DNA nanostructured surface through multivalent binding. **b** Electrocatalytic current was collected from 1000 MCF-7 cells

however, the aptamer specifically interacts with PrP^C and pushes TAMRA away from guanine, resulting in recovery of the quenched fluorescence.

The quenching efficiency was measured by the fluorescence intensity of TAMRA at 580 nm (Fig. 2b) [36]. The quenching efficiency was as high as 76.6 %, indicating that the proposed strategy successfully showed good applicability for the detection of PrP^C. Circular dichroism can be used to estimate the conformational change of the TAMRA-

containing aptamer because the spectrum depends on the conformation. In the absence of cDNA, the TAMRA-containing aptamer shows differences in the circular dichroism spectrum from that of its single-stranded cDNA as shown in Fig. 2c [36]. In addition, when the denatured TAMRA-containing aptamer was incubated with various concentrations of PrP^C, the recovered fluorescence intensity exhibited a linear relationship in a range from 1.1 to 44.7 g/mL with high correlation ($R=0.991$) and a low detection limit (0.3 g/mL).

Fig. 2 **a** The strategy for an aptamer-based fluorescence biosensor for detection of Cellular prion protein. **b** Fluorescence intensity of the tetramethylrhodamine (TAMRA)-containing aptamer in the neutral state (black line) and the thermally denatured state (red line), and that resulting from the hybridization with its complementary single-stranded DNA sequence (*cp-DNA*; green line) **c** Circular dichroism spectrum of the TAMRA-containing aptamer (black line), its complementary single-stranded DNA sequence (*cp-DNA*; red), and its hybrid with its complementary single-stranded DNA sequence (green line)



Alzheimer's disease (AD) is a degenerative disorder of the brain that accounts for most of the cases of dementia characterized by progressive cognitive impairment among people older than 65 years [47]. The neuropathological process of AD is associated with the formation of amyloid β ($A\beta$) peptide, also known as senile plaque, and neurofibrillary tangles of hyperphosphorylated tau protein have been used as biomarkers for early diagnosis [48]. There are two main strategies for the detection and quantification of these soluble AD biomarkers. The first strategy is the measurement of the total concentration of $A\beta$ or tau protein in cerebrospinal fluid (CSF) or plasma [49, 50]. However, this strategy showed unreliable results in terms of no significant differences in the levels of such markers between healthy individuals and AD patients [51]. The other strategy provided a more feasible solution, because it targets established pathogenic biomarkers such as cleaved tau protein, hyperphosphorylated tau protein, and $A\beta$ -derived diffusible ligands (ADDLs) [52–54]. However, in the early stage of the disease, the concentration of such markers in the CSF is extremely low, which makes it very hard to identify them accurately with conventional methods such as ELISA or blotting assays.

To solve this problem, Georganopoulou et al. [52] developed a new technique for highly sensitive detection of soluble AD biomarkers in CSF [53, 54]. In the method described in their work, ADDLs were recognized by magnetic microparticles with monoclonal anti-ADDL antibody attached, and then sandwiched with AuNPs functionalized with DNA barcode and polyclonal anti-ADDL antibody. The sandwich complexes were purified by magnetic separation (Fig. 3a). After repeated washing and dehybridization steps, a large number of DNA barcode strands were released, followed by isolation and quantification through a scanometric method. (Fig. 3a, b). By use of the silver amplification technique, ADDLs of subfemtomolar concentration were identified, and the detection sensitivity of the system was significantly enhanced by six orders of magnitude over the conventional ELISA method.

A calibration curve was obtained before the ADDL concentrations were analyzed in the subject samples (Fig. 3c) [52–54]. The assay exhibited a broad analytical concentration range from the order of 10^{-1} to 10^2 fM, with a detection limit as low as 100 aM. In addition, the signal plateau was achieved at higher ADDL concentrations (greater than 500 fM). As a result, the biobarcode assay can provide analytical detection of ADDLs from the lower attomolar to the upper femtomolar range. CSF samples obtained from AD patients and healthy individuals were used as a positive and a negative control, respectively (Fig. 3d). The ADDL concentration in the CSF was estimated by comparison of the grayscale intensity in the scanometric assay with the calibration curve. The median ADDL concentrations for the two groups were 200 aM and

1.7 fM, respectively ($P < 0.0001$, unpaired t test), which suggested that ADDL levels were significantly lower in the control group when compared with the AD group.

Infectious diseases

Hepatitis B is a devastating infectious disease caused by hepatitis B virus (HBV). Especially in Asian countries, a large number of patients are infected with HBV and the numbers are growing rapidly. Exposure to HBV can cause both acute and chronic inflammation of the liver, and consequently leads to cirrhosis and liver cancer [55, 56]. Therefore, it is necessary to develop a method for early HBV detection to possibly prevent disease progression. Recently, there have been many developments of methods for the detection of HBV, including chemiluminescence [57], spot hybridization [58], nested PCR [59, 60], reverse transcription PCR (RT-PCR) [61], and oligonucleotide-based biosensors [62, 63]. Although several PCR-based methods have been developed, these methods have several limitations owing to the lack of amplification specificity and the requirement for highly sophisticated equipment [64]. Thus, there is a growing need for the development of a new isothermal detection method with improved sensitivity and specificity, such as the use of nucleic acid sequence based amplification, sequence displacement amplification, RCA, or loop-based isothermal amplification. Furthermore, there has been increasing interest in the quartz crystal microbalance (QCM) analytical method for biosensing, because it can provide a rapid response, high sensitivity, and high stability associated with the operating frequency of quartz crystals.

For example, Yao et al. [65] have designed an RCA-based QCM biosensor that can be used to directly detect HBV genomic DNA. After the RCA reaction, amplified RCA products can hybridize with the captured probes immobilized on the gold electrode surface by covalent bonding (Fig. 4a, b) [65]. In the presence of the target sequence, they hybridize with the circular probe, which is subsequently ligated by *E. coli* DNA ligase (Fig. 4a) [65]. The circular probe is constructed with 5' and 3' terminal sequences complementary to the target DNA sequences. Thus, the ends of the circular probe can be joined together only when the circular probe is hybridized with a perfectly matched target sequence. With a single-base mismatch in the target sequence, the RCA reaction cannot be initiated and the QCM frequency shift signal cannot be observed. After formation of the circular probe, the primer sequence is isothermally extended to generate a long ssDNA sequence with use of $\Phi 29$ DNA polymerase by the RCA. Even a single-base mismatch strand can be differentiated from the target strand, with the two advantages of high amplification efficiency of $\Phi 29$ DNA polymerase and the remarkable precision of *E. coli* DNA ligase. The relationship between the QCM frequency shift and the concentrations of HBV strands was investigated in the optimized condition (Fig. 4c) [65]. A

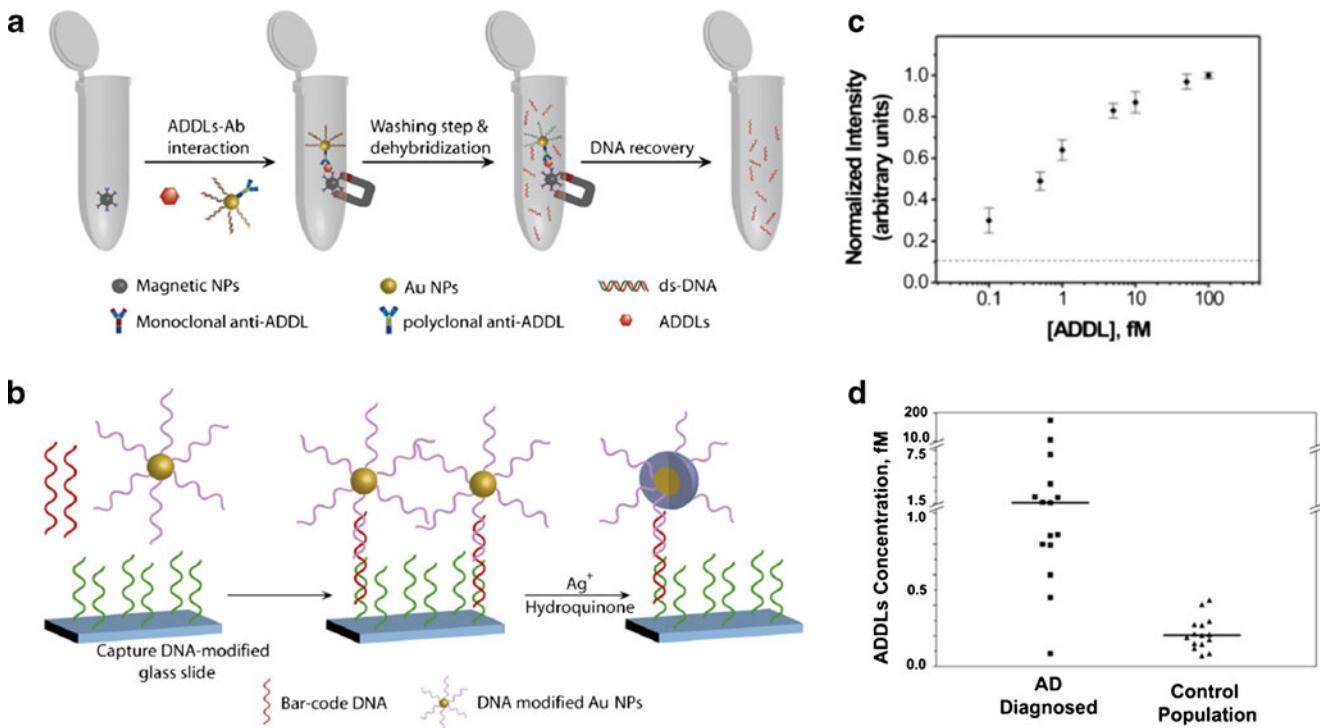


Fig. 3 **a** Amyloid β derived diffusible ligand (ADDL) detection by the biobarcode amplification assay. **b** The scanometric detection assay. **c** A normalized intensity curve for a series of serial ADDL concentrations. **d** Scatter plot of ADDL concentrations from the scanometric detection

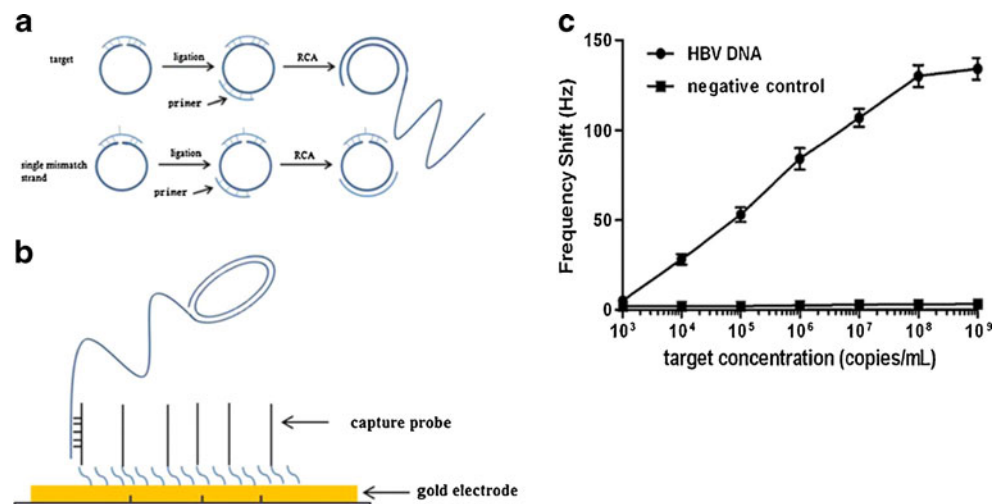
assay for patients with Alzheimer's disease (AD; positive control) and control subjects (negative control). *Ab* antibody, *ds-DNA* double-stranded DNA, *NPs* nanoparticles

positive linear relationship was observed between the two variables in the concentration range from 10^3 to 10^8 copies per milliliter, with a high correlation coefficient of 0.995. In addition, the frequency shift significantly increased along with the HBV target concentration over the range from 10^4 to 10^8 copies per milliliter. In contrast, there was an extremely low frequency shift in the control group, and virtually no increase in the frequency shift was observed over the same range.

The recent outbreaks of Ebola and Middle East respiratory syndrome were worldwide issues. Infectious diseases such as

Ebola, Middle East respiratory syndrome, and severe acute respiratory syndrome spread very quickly and easily. When outbreaks become pandemic, societies and their economies fall into chaos. It is necessary to detect these diseases early to prevent them from reaching epidemic status. RT-PCR is the most widely used method to diagnose infectious diseases. However, this method has multiple drawbacks. It requires a reverse transcription step for cDNA synthesis. Furthermore, a thermocycler is required for the annealing and amplification of target genes [66]. However, padlock probe recognition

Fig. 4 **a** Circular template hybridization with a target strand and a single-mismatch strand, respectively. After hybridization and ligation of the circular probe, rolling circle amplification (RCA) reaction was initiated. **b** The RCA product was immobilized on the gold electrode surface through hybridization with the capture probe. **c** The relationship between the frequency shift and target concentration (log scale) in the range from 10^3 to 10^9 copies per milliliter. *HBV* hepatitis B virus



shown in this system has various advantages. First, it has single-base specificity, meaning that it can distinguish a single base difference. Second, the amount of RCA product is directly proportional to recognition of the target pathogen because circularized molecular padlock probes formed only through recognition of the pathogen strand make the RCA product [67]. Furthermore, the direct proportional relationship between the RCA product and target recognition makes it possible to develop a biosensor with high sensitivity without an additional purification step [68]. The assay which uses the RCA reaction induced by the target pathogen can be implemented by simple modification of the surface of the device [69].

Here we describe an oligonucleotide-based biosensor for detection of infectious pathogens. The biosensor is called DhITACT, which stands for “DNA hydrogel formation by isothermal amplification of complementary target in fluidic channels” [70]. This system uses dumbbell-shaped padlock probes that can selectively hybridize with ssDNA/single-stranded RNA targets. After binding with pathogen strands, they form a closed circular structure by ligation and RCA can occur to generate long tandem repeats of DNA products. Once sufficient amplified DNA strands have been produced, they form self-entangled DNA hydrogels in microfluidic channels (DhITACT) with high viscosity. This results in selective blockage of matching channels with the target pathogen template (Fig. 5a). This system has good sensitivity relative to conventional RT-PCR. Complete blockage of flow can be visualized with the naked eye at 10 pM (6×10^9 copies per milliliter) and fluorescence detection results in a sensitivity of 0.1 pM (6×10^7 copies per milliliter) (Fig. 5b). All these processes happen at room temperature and require less than 3 h. This assay is a novel method which detects viral or bacterial DNA/RNA within a few hours by the naked eye.

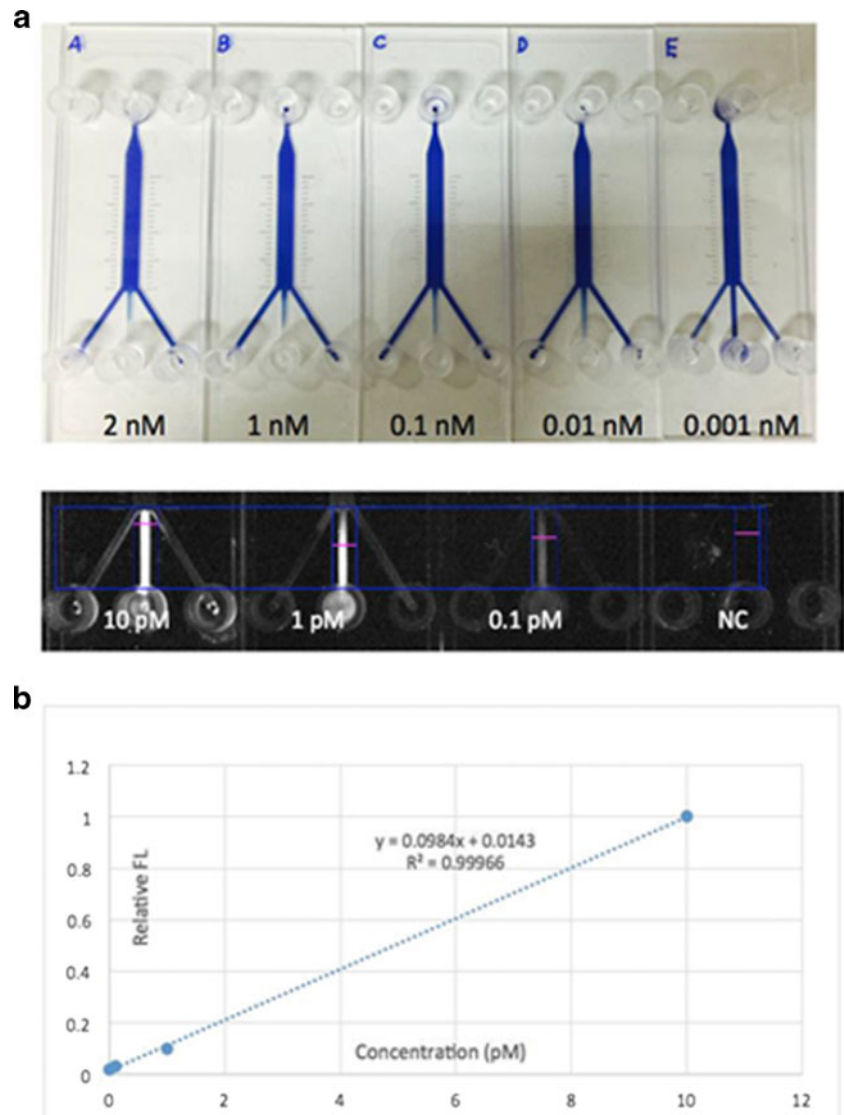
Biosensors for the detection of drugs in the body

A drug test is an analytical method for detecting illegal drugs or their metabolites in a human sample, such as a blood, sputum, or urine sample. Drug testing can be used in various situations. For example, it is used to detect prohibited drugs such as cocaine and steroids in sportsmen and sportswomen during competitions and outside competitions. Also, in everyday life, it measures the alcohol level in blood or breath air to catch drunken drivers. Among various drugs, cocaine addiction is a serious worldwide problem and cocaine is the second most used illegal substance in both Europe and the USA [71]. Multiple assays have been developed for the detection of cocaine, but most of these methods are time-consuming and require expensive laboratory equipment [72]. Therefore, the development of simple, sensitive, and rapid detection methods is necessary. For example, aptamers have been used as a new biosensor platform for the detection of cocaine.

Here we introduce examples of DNA-based biosensors for detection of cocaine. The first example uses quantum dots (QDs) immobilized with cocaine aptamer. The aptamer changes its shape from linear to hairpin when it binds to cocaine. That change causes Cy5 to be detached from QDs, resulting in the signal turning off. Therefore, the presence of cocaine can be determined by observation of the decrease of the Cy5 fluorescence signal [73]. QDs, which are semiconductor nanocrystals, have various advantages. For example, QDs have stable photoluminescence with a broad absorption range and a sharp emission range. In addition, they have adjustable photoluminescence for a similar reason [74]. QDs have been used as fluorescence resonance energy transfer (FRET) donors in many detection systems [38]. QDs can be used in a FRET detection system as novel and sensitive biosensors for cocaine. As shown in Fig. 6, if there is no cocaine, the Cy5 fluorescence signal can be detected because of FRET between 605QD and Cy5. Since QDs serve as FRET donors to provide energy to neighboring Cy5 molecules, strong Cy5 fluorescence signal can be obtained. As Fig. 6a shows, the presence of cocaine leads to the formation of a cocaine–aptamer complex and the associated conformation change results in the subsequent reduction of FRET between 605QD and Cy5. Time-correlated photon counting graphs showing fluorescence bursts depending on the existence of cocaine are presented in Fig. 6b. Figure 6b, graph A shows Cy5 and 605QD bursts from the 605QD–aptamer–Cy5 complex in the presence of cocaine. In contrast, there is no Cy5 signal in Fig. 6b, graph B because of the absence of Cy5 linked to the aptamer. Figure 6b, graph C shows the linear correlation of the Cy5 signal depending on the ratio of Cy5 and 605QD. Cy5 fluorescence signal reduction is observed depending on the concentration of cocaine (Fig. 6b, graph D). Greater reduction of the fluorescence signal is achieved with more cocaine.

Another cocaine detection system uses chemiluminescence-based cocaine aptasensors. Chemiluminescence is emission of light by a chemical reaction [75]. One example is emission of light by the reaction between luminol and hydrogen peroxide. Chemiluminescence analysis has various advantages, such as high sensitivity, cost-effectiveness, and simple but rapid detection. These merits make chemiluminescence analysis attractive as a detection tool [76]. Figure 7a outlines this approach. Magnetic microbeads coated with AuNPs are used for chemiluminescence detection of cocaine [77]. AuNPs provide a large surface area for enhanced immobilization of cocaine aptamer (S1) [78]. After immobilization of the cocaine aptamer (S1) on MB-AuNPs, the aptamer is hybridized with the signal DNA (S2) and HRP. This hybridization generates double-functional gold nanoprobe labeled with HRP. In the presence of cocaine, cocaine competes with signal DNA (S2) that is already bound to the cocaine aptamer. Since the binding between cocaine and cocaine aptamer is stronger than that between cocaine and signal DNA (S2), signal DNA (S2)

Fig. 5 The detection limit test of the DNA hydrogel formation by isothermal amplification of complementary target in fluidic channels (DhITACT) system by the dye solution method (a) and by the fluorescence detection method (b)



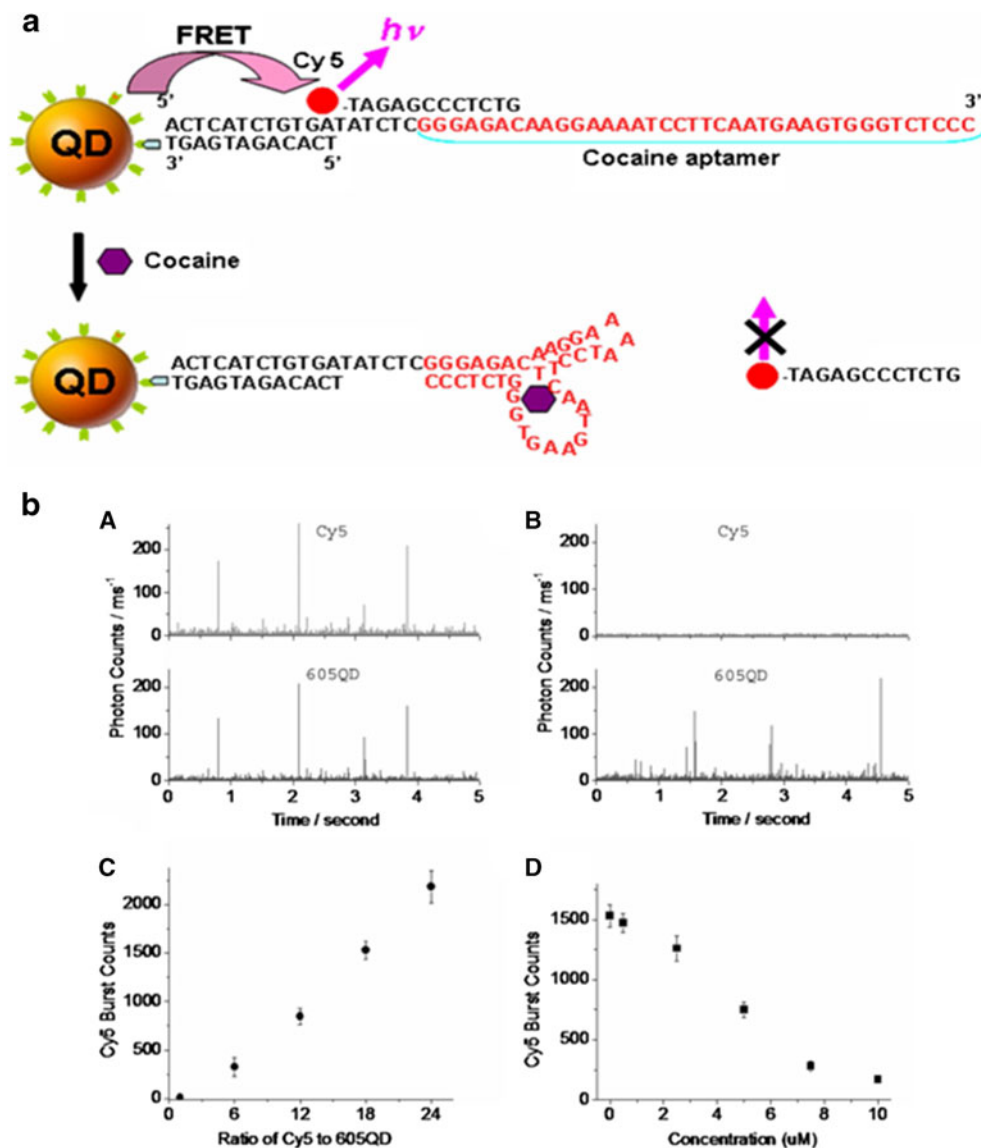
dissociates from the MB-AuNPs complex, which has cocaine aptamer attached. Free signal DNA (S2) conjugated with HRP can then react with luminol and H_2O_2 , generating a chemiluminescence signal. However, in the absence of cocaine, HRP cannot react with luminol and H_2O_2 because signal DNA (S2) conjugated with HRP is linked to magnetic microbeads (MB-AuNPs), meaning that it is not free and is in an unreactive state. The chemiluminescence signal of the luminol- H_2O_2 -HRP-*p*-iodophenol system has a linear relationship with the amount of cocaine (Fig. 7b, graph A). All these results were compared with those obtained without the use of AuNPs. The sensitivity of the aptasensor with AuNPs is much higher than that without use of AuNPs. Figure 7b, graph A outlines the relationship between the concentration of cocaine and the chemiluminescence signal with AuNPs, whereas Fig. 7b, graph B shows the relationship without AuNPs. The detection range of the assays with AuNPs is from 1.0×10^{-9} to 1.0×10^{-8} M in contrast to the method without AuNPs, which has

detection range from 1.0×10^{-8} to 1.0×10^{-7} M. The sensitivity of the biosensor with AuNPs is about ten times higher than that of assays without AuNPs.

Sportsmen and sportswomen should take a doping test during competitions such as the Olympic Games. Such a test detects the existence of prohibited substances in athletes' blood or urine. A doping list consists of banned drugs, stimulants, and hormones that enhance athletic performance artificially, and there is a need for rapid and accurate detection of various drugs on the doping list. Peptide hormones, growth factors, related substances, and mimetics are included in the major doping lists. For example, platelet-derived growth factor (PDGF) is a prohibited drug for athletes.

Yang et al. [79] developed a novel detection system for PDGF. This system uses RCA. A real-time amplification assay is suitable for detection and determination of PDGF. Currently, real-time PCR is a representative analytical method for many diagnostic applications [80]. However,

Fig. 6 Detection of cocaine with quantum dots labeled with cocaine aptamer. **a** Design of a biosensor using quantum dots labeled with cocaine aptamer. **b** Fluorescence signals from 605QD–aptamer–Cy5 complexes in various condition: Cy5 fluorescence signals from the 605QD–aptamer–Cy5 complex in the presence of cocaine (A); signal off in the absence of Cy5 linked to the aptamer (B); correlation of the Cy5 fluorescence signal depending on the ratio of Cy5 and 605QD (C); Cy5 fluorescence signal reduction depending on the concentration of cocaine (D). *FRET* fluorescence resonance energy transfer, *QD* quantum dot



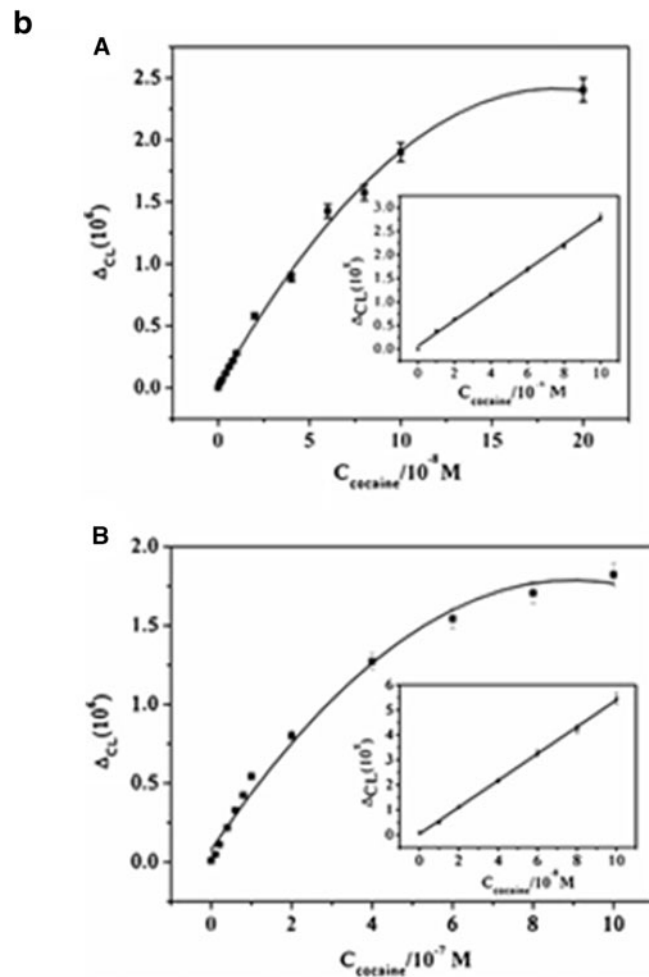
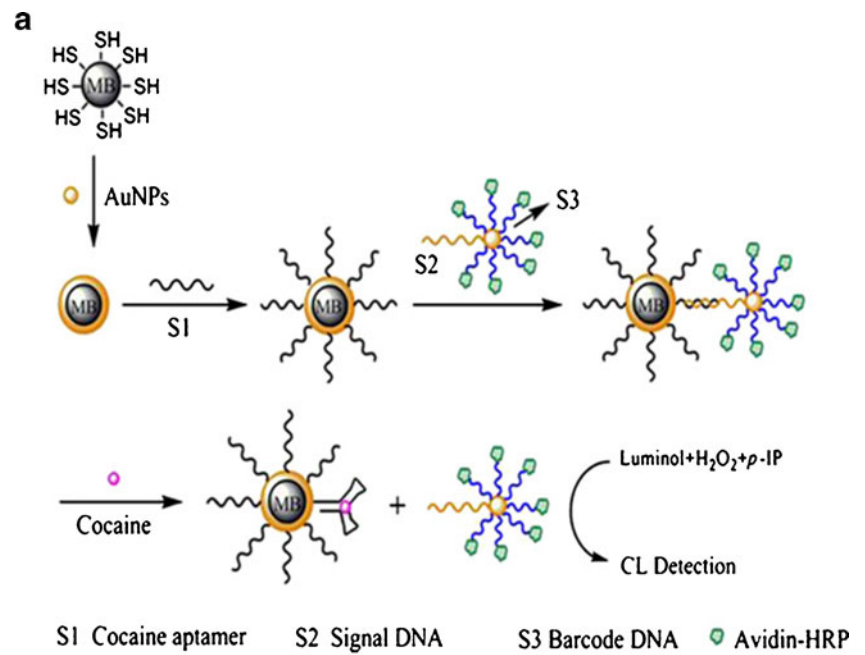
there is limitation in adjusting a RT-PCR system to an assay for proteins such as PDGF. Since they require an additional reverse transcription step, many RT-PCR methods are time-consuming. Instead, RCA can be used for the detection of target proteins [81]. Figure 8a shows a schematic plan of PDGF detection by RCA. To apply real-time RCA for PDGF detection, a conformation change of the aptamer is necessary for it to form a circularized template on interaction with its protein target (PDGF) [79]. Later, the circularized PDGF aptamer is recognized by the T4 DNA ligase, generating a closed circular loop for the RCA. Φ 29 DNA polymerase recognizes the 3' end of the primer, and continuously forms long oligonucleotide products. The RCA product can be detected by its binding with fluorescent nanoprobe [79]. The RCA product is massive, making possible its detection as discrete single molecules [82]. As in the conventional method, the real-

time RCA product can be detected by use of molecular beacons, cleavable probes, or SYBR Green [83]. With real-time RCA, it is possible to quantitate the amount of PDGF with a linear correlation. Figure 8b shows the quantitative relationship between fluorescence and two variables: reaction time and the concentration of PDGF in the sample. Both variables exhibit a linear relation with fluorescence intensity. This means that a longer reaction time and higher concentration of PDGF will result in a stronger fluorescence signal.

Oligonucleotide-based biosensors for detection of environmentally hazardous materials

People are receiving more exposure to hazardous materials, leading to excessive immune responses, cancer

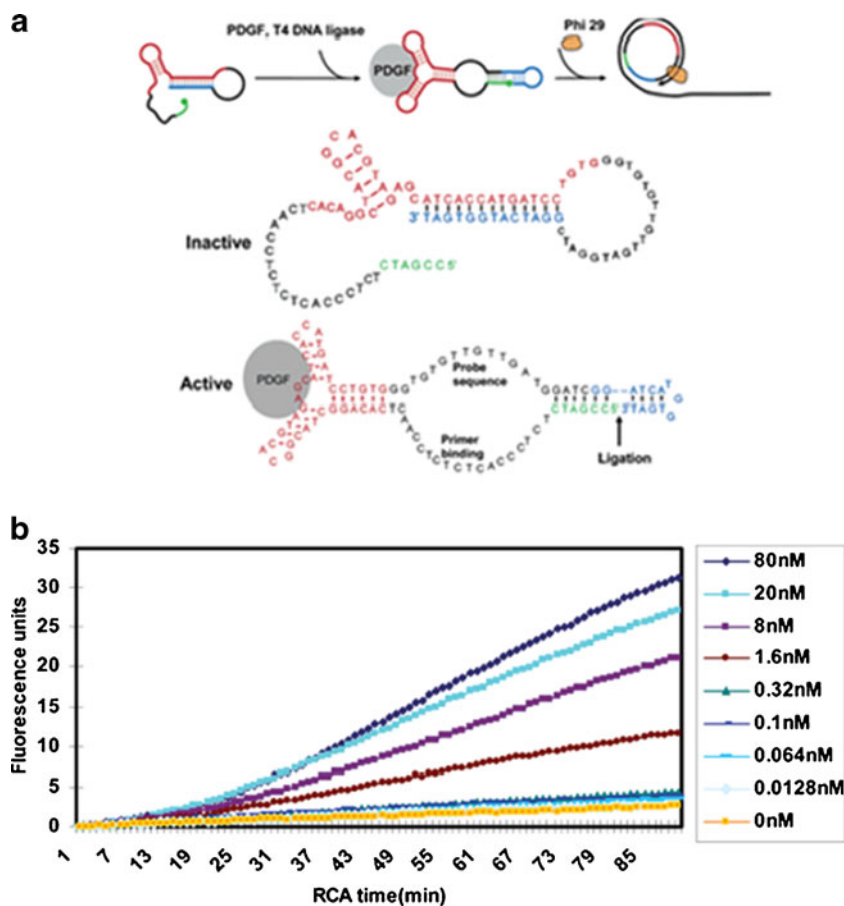
Fig. 7 a Cocaine detection using gold nanoparticles (*AuNPs*) with magnetic microbeads inside labeled with cocaine aptamer. **b** Chemiluminescence (*CL*) intensity depending on concentration of cocaine. *MB* magnetic microbead, *p-IP* *p*-iodophenol



development, imbalance of hormones, and abnormal early sexual development. To this end, early detection of

environmentally hazardous materials is of interest to many health care professionals and the public. There are many

Fig. 8 Platelet-derived growth factor (*PDGF*) detection by RCA. **a** General design principles for and design of the conformation-switching aptamer. **b** Fluorescence intensity depending on RCA time and protein concentration



hazardous materials around us in everyday life. For example, heavy metals, endocrine-disrupting hormones, antibiotics, and toxins are frequently found in standard products and in the environment. Among the heavy metals, mercury, lead, and cadmium are common. They induce toxicity through accumulation in the body. Mercury is toxic to the kidneys and induces anemia by hemolysis. Lead is toxic, especially to the nervous system. Heavy metals usually take a long time to cause health issues, but short-term exposure is a serious concern in developing countries. Endocrine-disrupting compounds (EDCs) include estradiol and bisphenol A (BPA; which acts as a hormone-mimicking substance), which cause an imbalance in the endocrine system, cancer development, and abnormal immune response in addition to reducing the reproductive capability of the individual. Tetracycline is a good example of a commonly used antibiotic. Animals or fishes are treated with antibodies to make them more resistant to diseases; however, antibiotics can accumulate in the human body over time with consumption of meat and fish products. Finally, aflatoxin B₁ and ochratoxin A (OTA) are toxins that cause food poisoning. It is easy to get food poisoning especially in warm and humid conditions, and it is important to detect toxins that can cause food poisoning.

Therefore, the detection of environmentally hazardous materials is very important for our protection.

Heavy metals: mercury, lead

Highly sensitive electrochemical sensors for lead(II) detection have been developed with use of multiwalled carbon nanotube (MWCNT)/AuNP-modified electrodes. Because of the Pb²⁺-induced guanine-rich DNA conformation, DNA aptamers can bind to Pb²⁺ ions with high sensitivity and selectivity. There are three types of DNA aptamers that can be used for the detection of Pb²⁺ ions: RNA-cleaving 8–17 DNAzyme [84], GR-5 DNAzyme [85], and Pb²⁺-dependent G-quadruplex (G4) oligonucleotide [86]. 8–17 DNAzyme and GR-5 DNAzyme show cleavage activity by catalyzing RNA transesterification when lead ions are present. The Pb²⁺-dependent allosteric G4 aptamer contains guanine-rich nucleic acid sequences, which allow G4 to form stacked arrays of G-quartets with a unique higher-order structure. Since the diameter of Pb²⁺ is smaller than that of many other ions, G4 offer an advantage because of their selectivity [87]. Conventionally used methods for detection of Pb²⁺ ions, such as atomic emission spectrometry and mass spectrometry, have some problems such as multiple sample preparation steps and limited

sensitivity. To overcome these barriers, fluorescent [75, 88, 89], electrochemical, photoelectrochemical, and optofluidic sensing strategies have been studied.

Recently, Zhu et al. [90] developed an electrochemical sensor for the detection of Pb^{2+} -dependent G4. Additionally, AuNPs and MWCNTs were introduced to improve the conductivity of biosensors. AuNPs and MWCNTs exhibit good electrical conductivity and large surface areas that are appropriate for electrochemical sensors. To construct MWCNT/AuNP-modified electrodes, MWCNTs were assembled on the surface of glassy carbon electrodes and AuNPs were coated. The DNA capture probe 5'-CACCCACCCAC-SH-3' was immobilized on the surface of the AuNPs via Au-SH interaction. When there are no Pb^{2+} ions in the sample, the DNA aptamer probe 5'-(GGGT)₄-3' can hybridize with the capture probe. In the presence of Pb^{2+} ions, the DNA aptamer probe reacts with lead ions, forming a highly stable G4 structure. As a result, methylene blue is detached from G4, resulting in reduced conductivity of the electrochemical sensor. The advantage of this platform compared with other electrochemical sensors is its improved sensitivity. Because of the highly conductive MWCNTs and AuNPs, it can detect very low concentrations of lead ions: the limit of detection is 4.3×10^{-15} M. Furthermore, it shows linearity with a range of 5.0×10^{-11} to 1.0×10^{-14} M.

Photoelectrochemistry is another good strategy for the detection of lead ions, owing to its low background signal and high sensitivity [91–93]. In the photoelectrochemistry sensing system, light excites some particles and induces a change in the photocurrent signal. Commonly, QDs are used for bioanalysis because of their resistance to photobleaching as well as their broad absorption spectrum and sharp emission spectrum [74]. As shown in Fig. 9a, ascorbic acid donates electrons to QDs and the photoelectric current generated can be measured in the presence or absence of lead ions. In the absence of lead ions, DNA aptamer can hybridize with the AuNP-labeled DNA strands and AuNPs can induce the quenching of the photoelectric current through an energy transfer between QDs and AuNPs. In contrast, when a sample containing Pb^{2+} ions is applied, Pb^{2+} interacts with the aptamer, forming the stable G4 structure [94]. Formation of the G4 structure inhibits the sequence-specific binding of the aptamer with the AuNP-labeled DNA strands, thereby maintaining a high photoelectric current signal. Figure 9b shows the linear relationship between the photocurrent and the concentration of lead ions. With increasing concentration of lead ions, the photocurrent increases. The photoelectrochemical sensor has a strong advantage, because it can handle the water sample directly from the environment without pretreatment. Compared with other detection methods, it has high selectivity for lead ions even with other ions in the sample such as potassium, nickel, cobalt, and sodium ions. Second, the sensor has a linear range from 1.0×10^{-10} to 5.0×10^{-8} M and the

limit of detection is 5×10^{-11} M, which is lower than that of other photoelectrochemistry-based sensors (Fig. 9c).

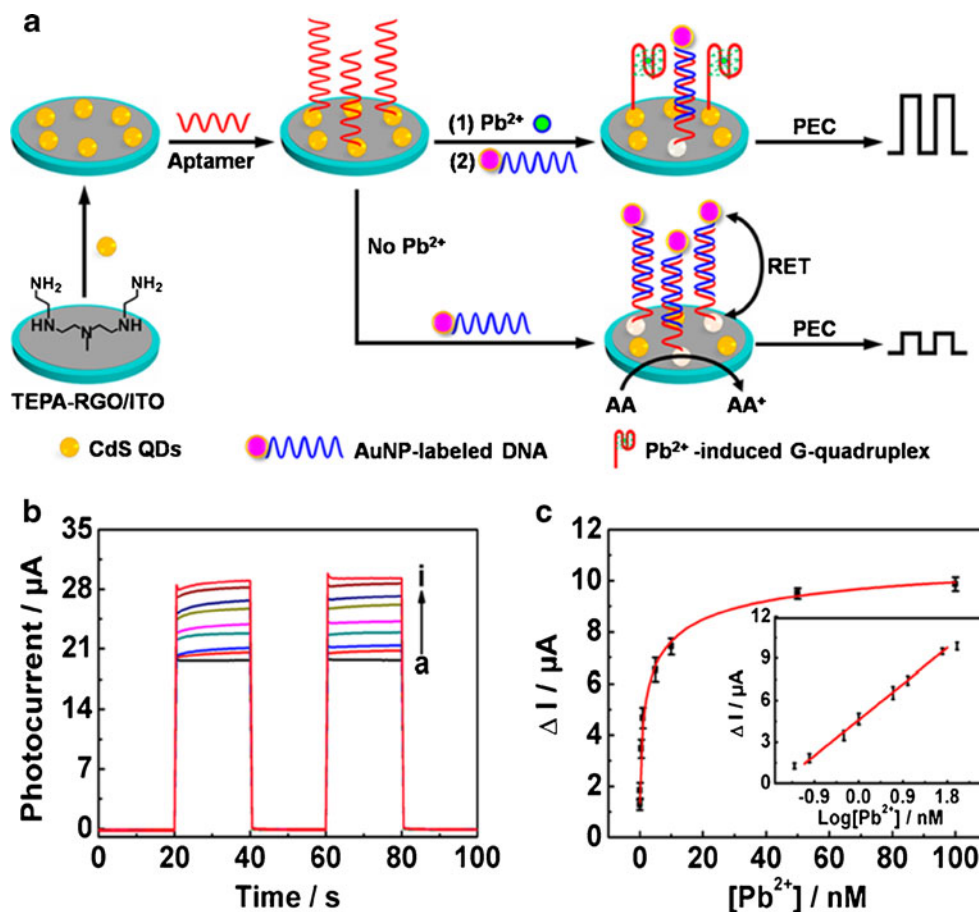
The third example of a Pb^{2+} biosensor uses an all-fiber optofluidic biosensing platform. A biosensor equipped with an optofluidic system can be very useful with real samples, because a very small volume of sample is required for detection of Pb^{2+} ions [95]. The all-fiber optofluidic biosensing system comprises four parts: a microfluidic system, an all-optical fiber system, a signal processing system, and a signal control system. When a pulsed laser beam (635 nm, 5 mW) is generated, it passes through the silica optical fiber coupler and reaches the tapered optical fiber sensor. An evanescent wave is produced at the surface of the optical fiber sensor and excites the immobilized fluorescently labeled G4 aptamer. Because of the narrow range of the evanescent wave, it is possible to discriminate bound aptamers from unbound aptamers without an additional washing step.

In this platform, the G4 aptamer is labeled with fluorescent Cy5.5 and is used as a recognition probe. Another DNA probe with a sequence complementary to the G4 aptamer is bound to the surface of the optical fiber sensor by a covalent bond. When there is a high concentration of Pb^{2+} ions in the optofluidic system, the fluorescence signal decreases because of competition for the immobilized cDNA probe between the G4 aptamer and the Pb^{2+} ions (Fig. 10a). Figure 10b shows the fluorescence signal during detection of Pb^{2+} using the optofluidic biosensor described. The fluorescence signal decreases with increasing concentration of Pb^{2+} , from 0 to 1 M. Figure 10c shows the relationship between the fluorescence signal and the calibration plot for the detection of Pb^{2+} . The optofluidic biosensor can achieve a linear range from 1.0 to 300.0 nM with the following equation: $I' = 0.305 \times \log[\text{Pb}^{2+}] + 0.0705$. The optofluidic-based aptasensor can offer simple and fast detection in water samples. As mentioned before, another beneficial point is the very small volume of sample needed for the analysis. In this platform, a 3.0- μL sample volume is enough for the detection process. Furthermore, reusability of the sensor probe is possible, allowing cost-effective measurement [96].

Mercury ions are very notorious environmentally toxic pollutants and are a global issue, because they cause severe and irreversible effects in human [97, 98]. To detect small amounts of mercury with high sensitivity, ssDNA aptamers with thymine residues can be used. When thymine-containing ssDNA encounter mercury ions, the mercury ions bind tightly between the two thymine residues of the DNA because of their high electron density [99]. As a result, a T-Hg²⁺-T complex is formed.

In addition to T-Hg²⁺-T complex formation, fluorescence polarization can be used as an appropriate detection tool. The basic principle of fluorescence polarization is the excitation of fluorescent elements using polarized radiation. After excitation of the fluorescent molecules, the emission returns to a

Fig. 9 Lead detection by a photoelectrochemical aptasensor. **a** General design scheme of the aptasensor with CdS QDs and AuNP-labeled aptamer based on the principle of resonance energy transfer (RET) between CdS QDs and AuNPs. An indium tin oxide (ITO) electrode was coated with reduced graphene oxide (RGO), and tetraethylenepentamine (TEPA) was bound to the surface of the electrode, which enhances the photocurrent reaction. Ascorbic acid (AA) acts as an electron donor in this platform. **b** Increasing photocurrent for the aptasensor analyzed at different concentrations of lead ions: from *a* to *i* 0, 0.05, 0.1, 0.5, 1.0, 5.0, 10, 50, and 100 nM. **c** Calibration curve of photocurrent versus the concentration of the lead ions. PEC photoelectric current



fixed plane [100]. Fluorescence polarization changes depending on the molecule's rotational relaxation time, increasing with longer rotational relaxation time. Shen et al. designed a biosensor involving an adapted fluorescence polarization system for the analysis of mercury ions [101]. To enhance the fluorescence polarization signal, iron oxide nanoparticles were selected as the magnetic core material. Iron oxide nanoparticles are commonly used as magnetic resonance imaging contrast agents [102]. As shown in Fig. 11a, a thymine-rich ssDNA probe is connected to superparamagnetic iron oxide nanoparticles through streptavidin–biotin linkage. Additional thymine-containing ssDNA is labeled with fluorescent dye for fluorescence polarization measurement. On the basis of the specific linkage between thymine and Hg²⁺, thymine-rich ssDNA on superparamagnetic iron oxide nanoparticles and free fluorescently labeled thymine-rich ssDNA are bridged through Hg²⁺. The formation of a T–Hg²⁺–T complex allows the fluorescently labeled ssDNA to bind to superparamagnetic iron oxide nanoparticles, thus increasing their molecular weight. In response to the increased molecular weight, the fluorescence polarization signal is also increased in the sample. When different concentrations of the Hg²⁺ sample were tested, the biosensor based on the fluorescence polarization method showed a linear relationship over the range

from 2.0 nM to 1.0 mM (Fig. 11b). The limit of detection was estimated to be 0.49 nM. Compared with previous studies, this study revealed a low limit of detection and a wide range of linearity. Furthermore, it is possible to reuse the magnetic particles with similar reproducibility for six cycles [103].

Zhang et al. [110] have proposed another heavy metal detection system for mercury ions. In their detection system, a novel surface-enhanced resonance Raman scattering (SERRS) method was applied. Biosensors with optical detection techniques such as colorimetric analysis [104], fluorescence detection [105–107], plasmon resonance spectroscopy [108], and surface enhanced Raman scattering [109] have been widely studied. However, the sensitivity of these measurement platforms was uncertain at low sample concentrations. Zhang et al. [110] improved the sensitivity by developing a SERRS-based Hg²⁺ sensor with a detection sensitivity of 1 pM. In their study, nanoporous gold (NPG) is introduced as a plasmonic element, and a thymine-rich ssDNA probe labeled with Cy5 is attached to NPG via SH functional groups (Fig. 12a). When there are no Hg²⁺ ions in the sample, the distance between Cy5 and NPG is short, resulting in increased Raman signal intensity from Cy5. On the addition of Hg²⁺ ions, thymine residues are linked via T–Hg²⁺–T interaction. Because strong and specific binding is formed between

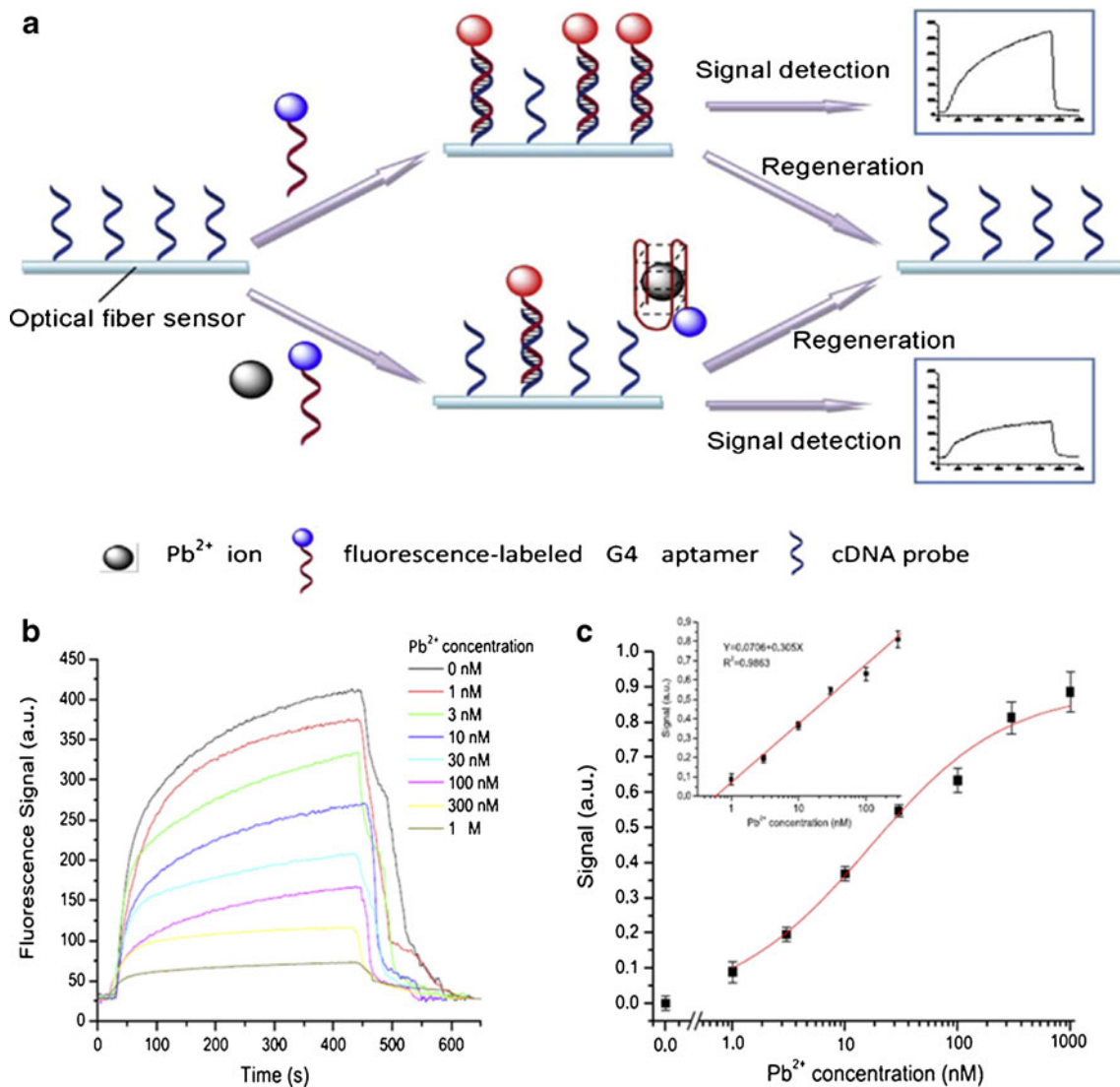


Fig. 10 Lead ion detection using an optofluidic aptasensor. **a** Scheme of the optofluidic aptasensor with a fluorescence-labeled aptamer. **b** Fluorescence signal of the aptasensor at different concentrations of lead ions ranging from

0 to 1 M. **c** Calibration curve of fluorescence signal versus the concentration of the lead ions. *cDNA* complementary DNA, *G4* G-quadruplex

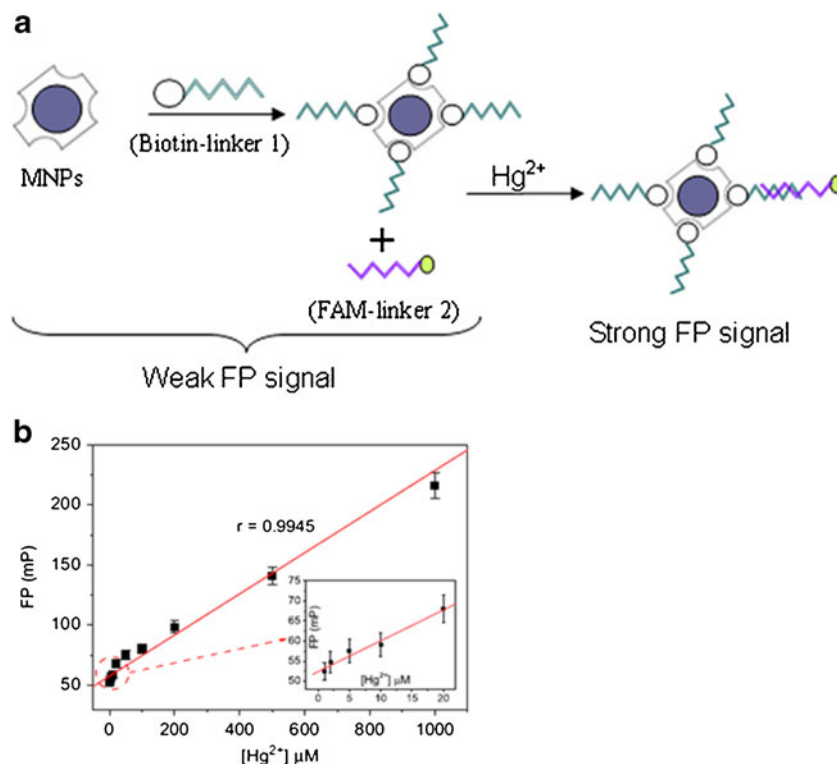
ssDNA aptamers, a strict duplex structure is observed. Unlike the flexible ssDNA aptamer, the distance between Cy5 and NPG increases when a strict duplex structure is formed. As a result, the local surface plasmon resonance effect of NPG is reduced as is the SERRS signal of Cy5. Figure 12b shows that the Raman intensity increases as the concentrations of Apt8@NPG decreases. The peak of the Raman intensity is at 1365 cm^{-1} . Since the distance between Cy5 and NPG is an important factor for the intensity of the SERRS signal, an appropriate thymine-containing aptamer is needed for appropriate sensitivity. It is reported that fewer thymine residues containing aptamer require fewer Hg^{2+} ions to form a rigid duplex structure. Therefore, aptamers containing a few thymine bases were used for highly sensitive detection. In this study, two kinds of aptamer, one containing 15 thymine bases (Apt15) and one containing eight thymine bases (Apt8), were

used to recognize the effect of aptamer length. Figure 12c shows the Apt8@NPG sensor is more sensitive than the Apt15@NPG sensor. It is noteworthy that the device is easily reusable after addition of 100 mM ascorbic solution for 1 h and washing for 15 min [111]. According to the reproducibility test result, the SERRS signal intensity varies within the range of 10 % for ten cycles [110].

Antibiotics: tetracycline

Tetracycline is a commonly prescribed antibiotic that inhibits protein synthesis for a broad spectrum of diseases. However, extensive use of tetracycline is a global issue as tetracycline residues remain in food products such as raw milk, meat, and honey. The residues can cause lethal side effects and allergic reactions in humans. Emerging

Fig. 11 **a** Scheme of a mercury ion detecting aptasensor using a T-Hg²⁺-T complex. **b** Fluorescence polarization (FP) of the aptasensor at different concentrations of mercury ions ranging from 2.0 nM to 20.0 μM. *MNPs* magnetic nanoparticles



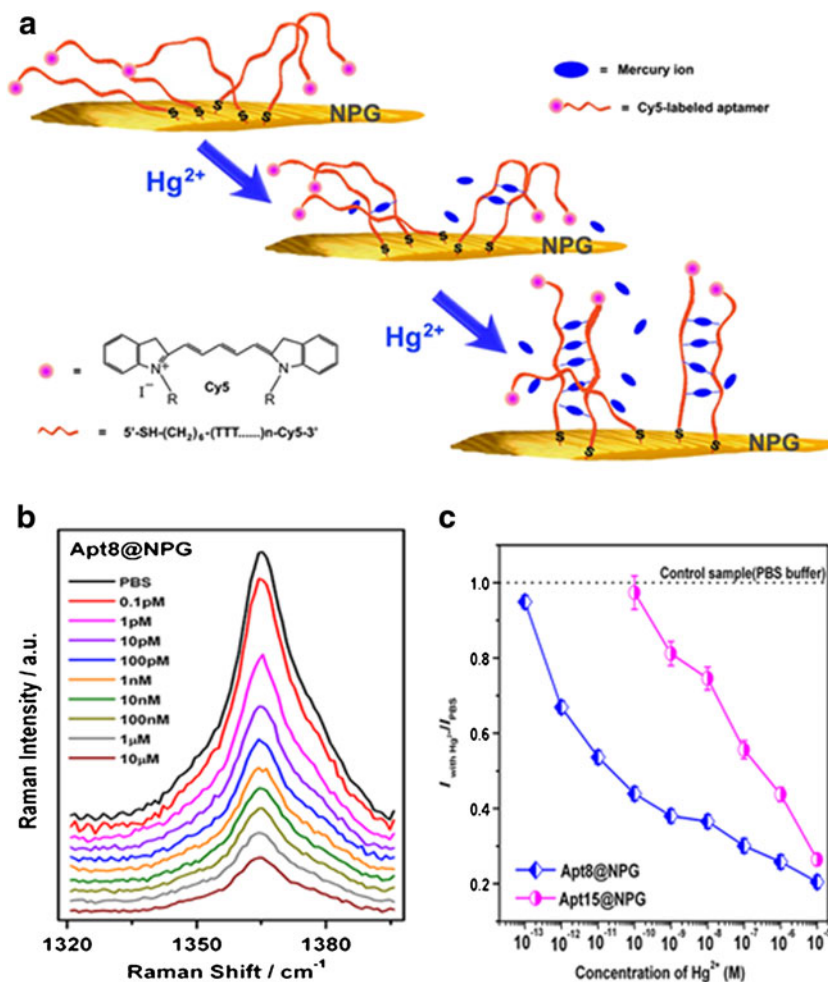
bacterial resistance to tetracycline is also considered a big problem. For these reasons, sensitive and selective analysis of tetracycline concentrations in food products has been studied.

Ramezani et al. [112] have designed a biosensor to detect tetracycline in milk that is based on a triple-helix molecular switch (THMS) system. The colorimetric THMS system has been used to detect other species, such as potassium ions, and this was the first time it was used for detection of tetracycline with AuNPs and aptamer [113]. The THMS system has remarkable features compared with the double-helix DNA aptamer in that it is much more stable and sensitive, with similar binding affinity [114]. In this study, the ssDNA aptamer 5'-CTCTCTCGGTGGTGTCTCTC-3' was used for high-affinity binding to tetracycline. Triple-helix structures consisting of aptamers and signal transduction probes were used for the detection of tetracycline. In the absence of tetracycline, the AuNPs become unstable and aggregate. Because the AuNPs changed from red to blue when the AuNPs formed aggregates, colorimetric detection of tetracycline was achieved. In the presence of tetracycline, aptamers bind to tetracycline instead of the signal transduction probe. The remaining signal transduction probes react with AuNPs and attach to the surface of AuNPs. As a result, AuNPs remain stable, avoiding aggregation. The sensors based on the THMS system have the ability to detect tetracycline in samples containing the antibiotic at a concentration of at least 266 pM (0.127 μg/L). In other studies, the limit of detection was

0.5 μg/L for high-performance liquid chromatography with UV detection [115], 2 μg/L for microbiological tests [116], 0.19 μg/L for immunoassays [117], and 2.4 μg/L for electrochemical aptasensors [118]. As the absorbance of AuNPs increases depending on the concentration of tetracycline, quantitative analysis of tetracycline is possible. The sensor shows a wide range of linearity from 0.3 nM to 10 nM for tetracycline, and can specifically react with tetracycline in mixtures with other antibiotics such as clindamycin, amoxicillin, and ciprofloxacin. Furthermore, the designed aptasensors can be directly applied to detect tetracyclines in real samples such as milk and serum. The maximum allowed concentration for tetracycline in milk is 0.1 mg/L, which is much higher than the limit of detection for aptasensors based on the THMS system [112].

For analysis of trace metal ions and small biological elements such as enzymes, proteins, and DNA, resonance scattering spectral analysis has been reported to exhibit high selectivity and sensitivity. Tao et al. [119] demonstrated that the resonance scattering spectral signal could be improved with the addition of an inorganic catalyst, which indicates the enhancement of sensitivity. For example, inorganic catalysts such as AuNPs have characteristics suitable for biosensors: high conductivity, catalytic activity, and biocompatibility. Single-stranded DNA (ssDNA) aptamers can be immobilized on the surface of AuNPs via van der Waals forces and stabilize the nanoparticles. Unlike aptamer-coated nanogold (ACNG), uncoated AuNPs aggregate and lose catalytic activity. Enhanced catalytic activity via the Fehling reaction rarely occurs

Fig. 12 **a** Scheme of a mercury ion detecting aptasensor based on the surface-enhanced resonance Raman scattering (SERRS) method. **b** Raman intensity of the aptasensor at different concentrations of mercury ions. **c** Raman intensity of the 1365-cm⁻¹ peak; the plot for the Apt15@NPG SERRS is shown for comparison. *NPG* nanoporous gold, *PBS* phosphate-buffered saline



before the temperature reaches 100 °C. However, the addition of ACNG induces the Fehling reaction following the reduction of Cu²⁺ and glucose to produce cubic Cu₂O at 60 °C.

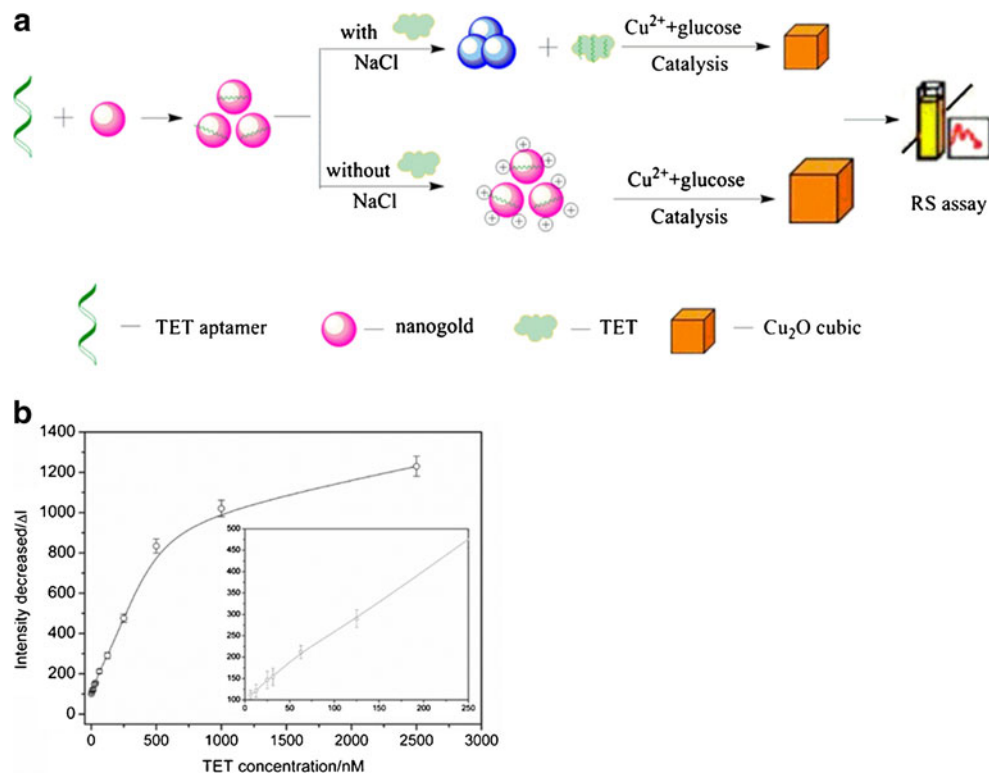
In addition, Luo et al. [120] designed an aptasensor using the resonance scattering spectral detection method with catalytic nanogold particles. Nanogold particles were modified and coated with tetracycline-binding ssDNA aptamers. Without tetracycline, the aptamer binds to the surface of the nanogold particles, which stabilizes the nanogold particles (Fig. 13a). The stabilized nanogold particles catalyze the Fehling reaction and generate a large amount of cubic Cu₂O, resulting in increased resonance scattering signal. With tetracycline, tetracycline binds to the aptamer and naked nanogold particles aggregate, reducing the magnitude of the Fehling reaction observed. As a small amount of cubic Cu₂O is produced, the resonance scattering signal decreases. In conclusion, the relationship between the amount of tetracycline and the resonance scattering signal is inversely proportional. The calibration curve for the ACNG resonance scattering method was obtained at 620 nm, at which cubic Cu₂O shows a significant peak. To observe the linearity range of the aptasensor, samples containing 0–2500 nM tetracycline were examined.

The resonance scattering signal at 620 nm decreased consistently as more tetracycline was added, up to 625 nM. Above a concentration of 625 nM, the calibration curve barely increased, indicating that the aptamers were saturated with tetracycline (Fig. 13b). The limit of detection was 11.6 nM, low enough for use in milk samples. The selectivity of the aptasensor has also been tested with antibiotics such as thiamphenicol, kanamycin, and aztreonam and small molecules such as tyrosine, valine, and lysine. When other molecules at 0.5 mM are individually added, the changes in the resonance scattering signal are all below 200 au. In comparison, tetracycline samples result in a change of about 900 au in the resonance scattering signal.

Fungal toxin : ochratoxin A

Food safety has drawn global attention, and food intoxication in particular is an increasing problem. Ochratoxin can have irreversible effects on human health, such as nephrotoxic, immunotoxic, teratogenic, and carcinogenic effects. Ochratoxin is categorized into three types: ochratoxin A (OTA), ochratoxin B, and ochratoxin C. The types have slightly

Fig. 13 **a** Aptamer-coated nanogold catalytic resonance scattering (RS) assay for detection of tetracycline (TET). **b** The calibration curve of the aptamer-coated nanogold tetracycline sensor shows the intensity of the resonance scattering signal decreases with increasing tetracycline concentration. The curve was obtained with a correlation of 0.998

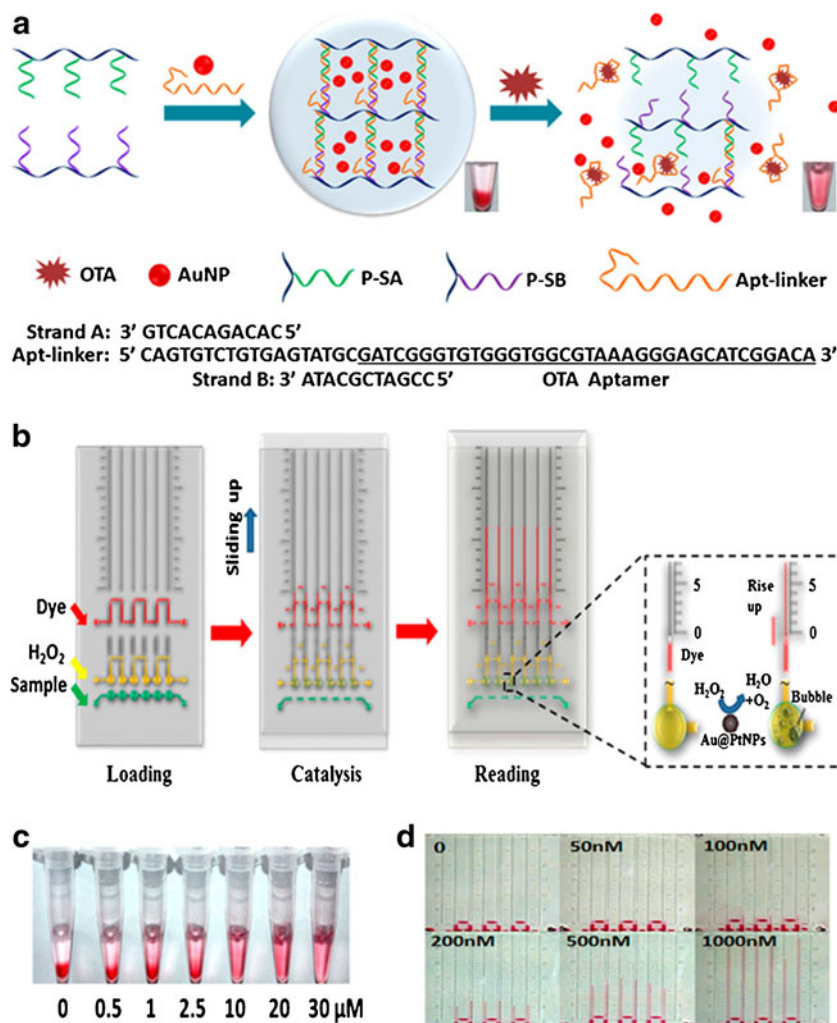


different chemical structures. Among the three subtypes, OTA is often found in food products including cereals, wheat, coffee beans, beer, and grape juice. The maximum permitted level of OTA in various food products was recently established: 3.0 ppb in cereals, and 2.0 ppb in beer and grape juice. To confirm and verify the permitted level, sensitive and selective detection methods without the use of complex and time-consuming instruments are required.

For this purpose, DNA hydrogels composed of DNA and aptamers are designed as biosensors and drug delivery systems [121, 122]. Hydrogels have several advantages, including stability, portability, low cost, and flexibility similar to natural tissue and exhibit a unique property in that they can swell and disintegrate depending on the surrounding environment. Because of these properties of hydrogels, Liu et al. [123] chose target-responsive DNA hydrogels as the basis for an OTA sensor. In their novel biosensor, an OTA aptamer is used as a linker strand (Apt-linker in Fig. 14a) and two kinds of DNA strands are attached to a linear polyacrylamide chain (Fig. 14a). The DNA strands contain sequences that are complementary to some parts of the aptamer used as a linker strand. For qualitative analysis, AuNPs are added to the hydrogel as indicator material. With OTA, DNA hydrogels dissociate because OTA binds with the aptamer used as a linker strand. As cross-linking between hydrogels collapses, preloaded AuNPs are released, which can be recognized easily by the naked eye. Figure 14b shows the reaction of the colorimetric OTA-detecting hydrogels with different

concentrations of OTA. The color of the supernatant gradually increases with increasing concentration of OTA. From analysis of the absorbance of AuNPs at 520 nm, a calibration curve can be obtained, with an upper limit of OTA concentration of 2.5 μM . The absorbance increases as the sample contains more OTA. This result corresponds well with the proposed detection mechanism, which assumes that decomposition of the hydrogel will release more free AuNPs. Quantitative detection as well as qualitative detection of OTA is achieved with a volumetric bar-chart chip (V-Chip) [124]. Instead of AuNPs, nanoparticles consisting of a gold core and a platinum shell (Au@PtNPs) are loaded. Au@PtNPs have high catalytic activity for decomposing H_2O_2 to O_2 , which can change the height of the ink bar. As more O_2 is produced by Au@PtNPs, the indicator on the ink bar goes up on the V-Chip. Figure 14c shows the V-Chip readout constructed with two glass slides and six parallel channels. Because of the scale marks on the parallel channels, quantitative detection is easy and simple. The supernatant including Au@PtNPs is loaded in the bottom lane and is unable to move into other lanes because only horizontal channels are connected. For the same reason, H_2O_2 is in the middle lane and the red ink is in the top lane. After loading, horizontal channels are disconnected and vertical channels are connected to make the sample react with H_2O_2 . Catalytic Au@PtNPs decompose H_2O_2 to produce O_2 . As the concentration of OTA increases, the distance moved by the red ink is greater. The linear relationship between the concentration of OTA and the distance moved by the red ink is

Fig. 14 Ochratoxin A (OTA) detection using aptamer-cross-linked hydrogel. **a** The principle behind the aptamer-cross-linked hydrogel for visual detection of OTA. With OTA, DNA hydrogels dissociate and preloaded AuNPs are released, which changes the color of the supernatant from colorless to red. **b** Quantitative detection of OTA with HV-Chip: aptamer-cross-linked hydrogel modified with volumetric a bar-chart chip for visual quantitative detection. **c** Images showing the decomposition of hydrogel in 120 min with different concentrations of OTA. **d** Images showing the linear relationship between ink movement and the concentration of OTA in the range from 0 to 1000 nM in 30 min. *PtNPs* platinum nanoparticles



shown in Fig. 14d. With the V-Chip, the sample containing OTA at a concentration ranging from 0 to 1 μM shows linearity with the height of the ink bar. The limit of detection with the V-Chip is 10.8 nM. This result shows that the sensitivity is highly improved by use of a V-Chip as compared with the previous detection method using AuNPs (0.24 μM). The DNA-hydrogel-based aptasensor is very promising because it is easy to handle, detection is simple, and it is able to distinguish between OTA and ochratoxin B.

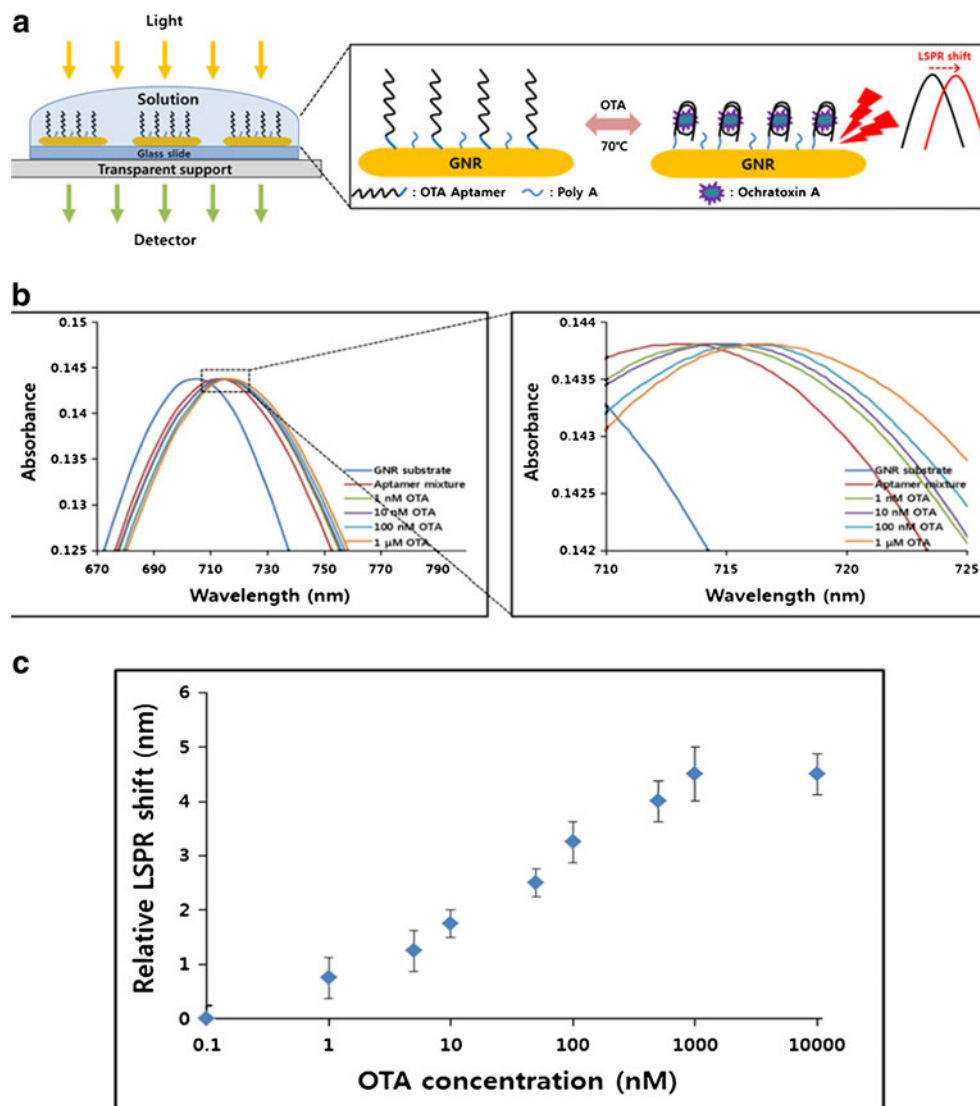
In another study, a localized surface plasmon resonance (LSPR) aptasensor was designed to detect OTA [125]. The LSPR-based aptasensor offers an easy, quick, and sensitive detection method based on the principle that a redshift of the LSPR band occurs when molecules are absorbed on the surfaces of nanoparticles, changing the refractive index. The LSPR aptasensor comprises glass, gold nanorods, and OTA-specific aptamers (Fig. 15a). An OTA-specific aptamer is tightly linked to the surface of the gold nanorod through thiol-gold interaction. When immobilized aptamers encounter OTA, the structure of the aptamer is changed, forming a G4 structure. Because of the stable G4 structure, the LSPR

aptasensor can resist relatively high temperatures, and the aptasensor can be reused several times if the temperature is increased to 70 $^{\circ}$ to remove bound OTA. The G4 structure also has the advantage of increasing the local density of the aptamer on the gold nanorod, enhancing the sensitivity of the LSPR aptasensor. The changed structure of the OTA aptamer leads to the redshift of the LSPR band, as the refractive index on the surface of the gold nanorod is changed. As a result, a redshift from 712.91 to 716.71 nm occurs with 1 μM OTA in the sample (Fig. 15b). To evaluate the linear relationship between the OTA concentration and the redshift of the LSPR band, different concentrations of OTA were added and analyzed. The calibration curve exhibits linearity in the range from 0.1 nM to 10 μM (Fig. 15c).

Endocrine disruptors

EDCs exist in everyday items such as plastic cups or dishes. EDCs such as BPA act similarly to the biological hormone estrogen. It can provoke precocious puberty and induce infertility [126]. Therefore, there is need for rapid and facile

Fig. 15 **a** Localized surface plasmon resonance (LSPR) OTA sensing system with a gold nanorod (GNR) and OTA-specific aptasensor. **b** Redshift of the absorbance obtained with different concentrations of OTA. **c** Relative LSPR peak shift for the OTA aptasensor with different concentrations of OTA from 0.1 nM to 10 μ M



detection of EDCs for production and regulatory practices. However, there are various limitations to the detection of EDCs. In reality, the environmental concentration of EDCs is too low for accurate detection [127]. In addition, EDCs exist mainly in complex mixtures with other materials, such as detergents and organic substances. To resolve these issues, multiple approaches have been adopted for the development of environmental biosensors for BPA [128]. BPA is an artificial organic material that is present in common plastic goods [129]. BPA is included in polycarbonate plastics as a plasticizer, which is an additive to increase flexibility and elasticity of plastics. There are various conventional analysis methods for the detection of BPA in portable water, such as high-performance liquid chromatography, gas chromatography–mass spectrometry, and liquid chromatography–mass spectrometry [129]. However, these existing methods have long detection times and analytical quantification is not accurate at a low concentration of BPA. In contrast to old methods, there

is a novel sensor for detection of BPA in portable water. This assay is based on surface-enhanced Raman scattering using gold–silver core–shell nanoparticles labeled with double-stranded DNA. The double-stranded DNA consists of Cy3-labeled BPA aptamer and thiolated probe DNA. In the presence of BPA, BPA binds with BPA aptamer instead of probe DNA, inducing Cy3 signal reduction. This analytical method is highly sensitive, having a limit of detection of 10 fM, and a detection range from 100 nM to 10 fM. It is 100–1000 times more sensitive than conventional methods.

Conclusion

This review has highlighted various oligonucleotide-based biosensors for medical diagnosis, crime detection, food analysis, and environmental field monitoring. Current molecular diagnostic methods such as ELISA and PCR have many

limitations because of complicated, expensive, and time-consuming procedures. Therefore, there remains a need for the development of novel biosensors with facile, rapid, and sensitive detection. As an alternative approach, oligonucleotide-based biosensors have drawn tremendous attention because of their unique advantages of having the dual role of simultaneous detection and amplification of target analytes. However, there are also inevitable drawbacks of oligonucleotide-based biosensors. First, many of these biosensors need temperature control for the detection and amplification of the target analyte. This requires equipment for temperature control such as a thermal cycler. Second, many of the detection methods are based on fluorescence detection. This requires the use of nucleic acid binding dyes and additional equipment for image analysis. Conventional PCR analysis is a good example, showing the aforementioned disadvantages.

Recently, there have been various efforts to overcome these limitations. One of them is the nucleic acid detection system that uses an isothermal amplification method such as RCA. This isothermal amplification does not require any equipment to control the reaction temperature. In addition, because of the repeated amplification or generation of the designed template, long chains of oligonucleotide can be produced, and their self-assembly and self-entanglement can induce the formation of a highly swollen network structure such as hydrogel. This allows non-fluorescence-based optical detection without the help of any equipment [70]. Such progress in oligonucleotide-based biosensors offers promise for the design of ideal diagnostic devices. Nonetheless, clinical applications are still rare, because there are many limitations in adapting the laboratory devices to real clinical diagnostic applications.

To overcome this bottleneck, the following requirements are necessary for clinical applications. First, it is very important to develop highly sensitive biosensors. Oligonucleotide-based biosensor can be a suitable candidate in this regard because of their high recognition ability and high binding affinity. Second, high selectivity is required for many in vitro diagnostics. This is a major obstacle in the clinical applications of biosensors. Although many biosensors work very well in a laboratory setup, many of them fail to analyze real serum samples from patients because of the lack of specificity. Therefore, it is important to develop highly specific and selective biosensors which can differentiate the small differences among tested samples. It is well known that oligonucleotide-based biosensors have clear advantage for sequence-specific detection of genes. However, the specificity of aptamer-based biosensors still needs to be improved. Lastly, multiplexing of detection is a key for saving analysis time. Especially, it is critical for clinical and environmental applications dealing with many samples with different target markers. To this end, we believe oligonucleotide-based biosensors can be an excellent platform technology for in vitro diagnostic applications and for the detection of environmentally hazardous

materials. Overall, we have shown that oligonucleotide-based biosensors have enormous potential to ensure the new era of facile, accurate, and cost-effective in vitro diagnostics.

Acknowledgments I.Y.J. and E.H.L. and A.Y.S. contributed equally to this work. This work was supported by the Basic Science Research Program (2012R1A1A1A05027352), The National Research Foundation of South Korea: BioMedical Technology Development Program (2015M3A9D7031026), and the Basic Science Research Program through the National Research Foundation of Korea funded by the Ministry of Science, ICT & Future Planning (NRF-2013K2A2A6000467)

Compliance with ethical standard

Conflict of interest The authors declare that they have no conflict of interest.

References

- Blum LJ, Coulet PR (eds) (1991) *Biosensor principles and applications*. Bioprocess technology, vol 15. Dekker, New York
- Hasan A, Nurunnabi M, Morshed M, Paul A, Polini A, Kuila T, Al Harii M, Lee YK, Jaffa AA (2014) Recent advances in application of biosensors in tissue engineering. *BioMed Res Int* 2014: 307519. doi:10.1155/2014/307519
- Maruthappu M, Williams C (2013) The biomarket. *Glob Public Health* 8(1):106–119. doi:10.1080/17441692.2012.758300
- Huang H, Zhu JJ (2009) DNA aptamer-based QDs electrochemiluminescence biosensor for the detection of thrombin. *Biosens Bioelectron* 25(4):927–930. doi:10.1016/j.bios.2009.08.008
- Khan A, Khan AA, Asiri AM, Rub MA, Azum N, Rahman MM, Khan SB, Ghani SA (2013) A new trend on biosensor for neurotransmitter choline/acetylcholine—an overview. *Appl Biochem Biotechnol* 169(6):1927–1939. doi:10.1007/s12010-013-0099-0
- Alix-Panabieres C, Pantel K (2013) Circulating tumor cells: liquid biopsy of cancer. *Clin Chem* 59(1):110–118. doi:10.1373/clinchem.2012.194258
- Nagrath S, Sequist LV, Maheswaran S, Bell DW, Irimia D, Utkus L, Smith MR, Kwak EL, Digumarthy S, Muzikansky A, Ryan P, Balis UJ, Tompkins RG, Haber DA, Toner M (2007) Isolation of rare circulating tumour cells in cancer patients by microchip technology. *Nature* 450(7173):1235–1239. doi:10.1038/nature06385
- Yoon HJ, Kim TH, Zhang Z, Azizi E, Pham TM, Paoletti C, Lin J, Ramnath N, Wicha MS, Hayes DF, Simeone DM, Nagrath S (2013) Sensitive capture of circulating tumour cells by functionalized graphene oxide nanosheets. *Nat Nanotechnol* 8(10):735–741. doi:10.1038/nnano.2013.194
- Williams SC (2013) Circulating tumor cells. *Proc Natl Acad Sci U S A* 110(13):4861. doi:10.1073/pnas.1304186110
- Plaks V, Koopman CD, Werb Z (2013) Cancer. Circulating tumor cells. *Science* 341(6151):1186–1188. doi:10.1126/science.1235226
- Yu M, Bardia A, Wittner BS, Stott SL, Smas ME, Ting DT, Isakoff SJ, Ciciliano JC, Wells MN, Shah AM, Conannon KF, Donaldson MC, Sequist LV, Brachtel E, Sgroi D, Baselga J, Ramaswamy S, Toner M, Haber DA, Maheswaran S (2013) Circulating breast tumor cells exhibit dynamic changes in epithelial and mesenchymal composition. *Science* 339(6119):580–584. doi:10.1126/science.1228522

12. Wen CY, Wu LL, Zhang ZL, Liu YL, Wei SZ, Hu J, Tang M, Sun EZ, Gong YP, Yu J, Pang DW (2014) Quick-response magnetic nanospheres for rapid, efficient capture and sensitive detection of circulating tumor cells. *ACS Nano* 8(1):941–949. doi:10.1021/nn405744f
13. Jiang X, Jiang Z, Xu T, Su S, Zhong Y, Peng F, Su Y, He Y (2013) Surface-enhanced Raman scattering-based sensing in vitro: facile and label-free detection of apoptotic cells at the single-cell level. *Anal Chem* 85(5):2809–2816
14. Liu H, Xu S, He Z, Deng A, Zhu JJ (2013) Supersandwich cytosensor for selective and ultrasensitive detection of cancer cells using aptamer-DNA concatamer-quantum dots probes. *Anal Chem* 85(6):3385–3392. doi:10.1021/ac303789x
15. Medley CD, Bamrungsap S, Tan W, Smith JE (2011) Aptamer-conjugated nanoparticles for cancer cell detection. *Anal Chem* 83(3):727–734. doi:10.1021/ac102263v
16. Park JM, Lee JY, Lee JG, Jeong H, Oh JM, Kim YJ, Park D, Kim MS, Lee HJ, Oh JH, Lee SS, Lee WY, Huh N (2012) Highly efficient assay of circulating tumor cells by selective sedimentation with a density gradient medium and microfiltration from whole blood. *Anal Chem* 84(17):7400–7407. doi:10.1021/ac3011704
17. Wu Y, Xue P, Kang Y, Hui KM (2013) Highly specific and ultrasensitive graphene-enhanced electrochemical detection of low-abundance tumor cells using silica nanoparticles coated with antibody-conjugated quantum dots. *Anal Chem* 85(6):3166–3173. doi:10.1021/ac303398b
18. Xu Y, Phillips JA, Yan J, Li Q, Fan ZH, Tan W (2009) Aptamer-based microfluidic device for enrichment, sorting, and detection of multiple cancer cells. *Anal Chem* 81(17):7436–7442. doi:10.1021/ac9012072
19. Yang X, Li J, Pei H, Zhao Y, Zuo X, Fan C, Huang Q (2014) DNA-gold nanoparticle conjugates-based nanoplasmonic probe for specific differentiation of cell types. *Anal Chem* 86(6):3227–3231. doi:10.1021/ac500381e
20. Yin J, He X, Wang K, Xu F, Shangguan J, He D, Shi H (2013) Label-free and turn-on aptamer strategy for cancer cells detection based on a DNA-silver nanocluster fluorescence upon recognition-induced hybridization. *Anal Chem* 85(24):12011–12019. doi:10.1021/ac402989u
21. Zheng T, Fu JJ, Hu L, Qiu F, Hu M, Zhu JJ, Hua ZC, Wang H (2013) Nanoarchitected electrochemical cytosensors for selective detection of leukemia cells and quantitative evaluation of death receptor expression on cell surfaces. *Anal Chem* 85(11):5609–5616. doi:10.1021/ac400994p
22. Maltez-da Costa M, de la Escosura-Muniz A, Nogues C, Barrios L, Ibanez E, Merkoci A (2012) Simple monitoring of cancer cells using nanoparticles. *Nano Lett* 12(8):4164–4171. doi:10.1021/nl301726g
23. Wu Y, Sefah K, Liu H, Wang R, Tan W (2010) DNA aptamer-micelle as an efficient detection/delivery vehicle toward cancer cells. *Proc Natl Acad Sci U S A* 107(1):5–10. doi:10.1073/pnas.0909611107
24. Zhou G, Lin M, Song P, Chen X, Chao J, Wang L, Huang Q, Huang W, Fan C, Zuo X (2014) Multivalent capture and detection of cancer cells with DNA nanostructured biosensors and multi-branched hybridization chain reaction amplification. *Anal Chem* 86(15):7843–7848. doi:10.1021/ac502276w
25. Xu JZ, Zhu JJ, Wu Q, Hu Z, Chen HY (2003) An amperometric biosensor based on the coimmobilization of horseradish peroxidase and methylene blue on a carbon nanotubes modified electrode. *Electroanalysis* 15(3):219–224
26. Veitch NC (2004) Horseradish peroxidase: a modern view of a classic enzyme. *Phytochemistry* 65(3):249–259
27. Soleymani L, Fang Z, Sargent EH, Kelley SO (2009) Programming the detection limits of biosensors through controlled nanostructuring. *Nat Nanotechnol* 4(12):844–848. doi:10.1038/nnano.2009.276
28. Li D, Song S, Fan C (2010) Target-responsive structural switching for nucleic acid-based sensors. *Acc Chem Res* 43(5):631–641. doi:10.1021/ar900245u
29. Tang Y, Ge B, Sen D, Yu HZ (2014) Functional DNA switches: rational design and electrochemical signaling. *Chem Soc Rev* 43(2):518–529. doi:10.1039/c3cs60264h
30. Grunnet M, Sorensen JB (2012) Carcinoembryonic antigen (CEA) as tumor marker in lung cancer. *Lung Cancer* 76(2):138–143. doi:10.1016/j.lungcan.2011.11.012
31. Duffy MJ (2001) Carcinoembryonic antigen as a marker for colorectal cancer: is it clinically useful? *Clin Chem* 47(4):624–630
32. Bohunicky B, Mousa SA (2011) Biosensors: the new wave in cancer diagnosis. *Nanotechnol Sci Appl* 4:1–10
33. Beveridge RA, Chan DW, Bruzek D, Damron D, Bray KR, Gaur PK, Ettinger DS, Rock RC, Shurbaji MS, Kuhajda FP (1988) A new biomarker in monitoring breast cancer: CA 549. *J Clin Oncol* 6(12):1815–1821
34. Liang K, Zhai S, Zhang Z, Fu X, Shao J, Lin Z, Qiu B, Chen G (2014) Ultrasensitive colorimetric carcinoembryonic antigen biosensor based on hyperbranched rolling circle amplification. *Analyst* 139(17):4330–4334
35. Wu Z-S, Zhou H, Zhang S, Shen G, Yu R (2010) Electrochemical aptameric recognition system for a sensitive protein assay based on specific target binding-induced rolling circle amplification. *Anal Chem* 82(6):2282–2289
36. Xiao SJ, Hu PP, Li YF, Huang CZ, Huang T, Xiao GF (2009) Aptamer-mediated turn-on fluorescence assay for prion protein based on guanine quenched fluophor. *Talanta* 79(5):1283–1286
37. Zhang DY, Zhang W, Li X, Konomi Y (2001) Detection of rare DNA targets by isothermal ramification amplification. *Gene* 274(1):209–216
38. Cheng Y, Zhang X, Li Z, Jiao X, Wang Y, Zhang Y (2009) Highly sensitive determination of microRNA using target-primed and branched rolling-circle amplification. *Angew Chem* 121(18):3318–3322
39. Aguzzi A, Calella AM (2009) Prions: protein aggregation and infectious diseases. *Physiol Rev* 89(4):1105–1152
40. Kocisko DA, Come JH, Priola SA, Chesebro B, Raymond GJ, Lansbury PT, Caughey B (1994) Cell-free formation of protease-resistant prion protein. *Nature* 370(6489):471–474. doi:10.1038/370471a0
41. Xiao S, Ou-Yang Y, Zhang X, Li X, Yang S, Chen H (2012) Aptamer-based assay for prion diseases diagnostic. *Procedia Environ Sci* 12:1348–1353
42. Gilch S, Schätzl HM (2009) Aptamers against prion proteins and prions. *Cell Mol Life Sci* 66(15):2445–2455
43. Sekiya S, Noda K, Nishikawa F, Yokoyama T, Kumar PK, Nishikawa S (2006) Characterization and application of a novel RNA aptamer against the mouse prion protein. *J Biochem* 139(3):383–390
44. Sekiya S, Nishikawa F, Noda K, Kumar P, Yokoyama T, Nishikawa S (2005) In vitro selection of RNA aptamers against cellular and abnormal isoform of mouse prion protein. *Nucleic Acids Symp Ser* 49(1):361–362
45. Gilch S, Kehler C, Schätzl HM (2007) Peptide aptamers expressed in the secretory pathway interfere with cellular PrP^{Sc} formation. *J Mol Biol* 371(2):362–373
46. Safar JG, Kellings K, Serban A, Groth D, Cleaver JE, Prusiner SB, Riesner D (2005) Search for a prion-specific nucleic acid. *J Virol* 79(16):10796–10806
47. Querfurth HW, LaFerla FM (2010) Alzheimer's disease. *N Engl J Med* 362(4):329–344. doi:10.1056/NEJMra0909142
48. Blennow K (2004) Cerebrospinal fluid protein biomarkers for Alzheimer's disease. *NeuroRx* 1(2):213–225

49. Clark CM, Xie S, Chittams J, Ewbank D, Peskind E, Galasko D, Morris JC, McKeel DW, Farlow M, Weitlauf SL (2003) Cerebrospinal fluid tau and β -amyloid: how well do these biomarkers reflect autopsy-confirmed dementia diagnoses? *Arch Neurol* 60(12):1696–1702
50. Blennow K, Hampel H (2003) CSF markers for incipient Alzheimer's disease. *Lancet Neurol* 2(10):605–613
51. Teunissen C, De Vente J, Steinbusch H, De Bruijn C (2002) Biochemical markers related to Alzheimer's dementia in serum and cerebrospinal fluid. *Neurobiol Aging* 23(4):485–508
52. Georganopoulou DG, Chang L, Nam J-M, Thaxton CS, Mufson EJ, Klein WL, Mirkin CA (2005) Nanoparticle-based detection in cerebral spinal fluid of a soluble pathogenic biomarker for Alzheimer's disease. *Proc Natl Acad Sci U S A* 102(7):2273–2276
53. Keating CD (2005) Nanoscience enables ultrasensitive detection of Alzheimer's biomarker. *Proc Natl Acad Sci U S A* 102(7):2263–2264
54. Brambilla D, Le Droumaguet B, Nicolas J, Hashemi SH, Wu L-P, Moghimi SM, Couvreur P, Andrieux K (2011) Nanotechnologies for Alzheimer's disease: diagnosis, therapy, and safety issues. *Nanomedicine* 7(5):521–540
55. Perz JF, Armstrong GL, Farrington LA, Hutin YJ, Bell BP (2006) The contributions of hepatitis B virus and hepatitis C virus infections to cirrhosis and primary liver cancer worldwide. *J Hepatol* 45(4):529–538
56. Shepard CW, Simard EP, Finelli L, Fiore AE, Bell BP (2006) Hepatitis B virus infection: epidemiology and vaccination. *Epidemiol Rev* 28(1):112–125
57. Young K-C, Chang T-T, Hsiao W-C, Cheng P-N, Chen S-H, Jen C-M (2002) A reverse-transcription competitive PCR assay based on chemiluminescence hybridization for detection and quantification of hepatitis C virus RNA. *J Virol Methods* 103(1):27–39
58. Fagan EA, Guarner P, Perera SD, Trowbridge R, Rolando N, Davison F, Williams R (1985) Quantitation of hepatitis B virus DNA (HBV DNA) in serum using the spot hybridization technique and scintillation counting. *J Virol Methods* 12(3):251–262
59. Almeida RP, Cardoso DD (2006) Detection of HBV DNA by nested-PCR in a HBsAg and anti-HBc negative blood bank donor. *J Clin Virol* 36(3):231–234
60. Vincenti D, Solmone M, Garbuglia AR, Iacomi F, Capobianchi MR (2009) A sensitive direct sequencing assay based on nested PCR for the detection of HBV polymerase and surface glycoprotein mutations. *J Virol Methods* 159(1):53–57
61. Mei SD, Yatsuhashi H, del Carmen PM, Hamada R, Fujino T, Matsumoto T, Inoue O, Koga M, Yano M (2000) Detection of HBV RNA in peripheral blood mononuclear cells in patients with and without HBsAg by reverse transcription polymerase chain reaction. *Hepatol Res* 18(1):19–28
62. Cha BH, Lee S-M, Park JC, Hwang KS, Kim SK, Lee Y-S, Ju B-K, Kim TS (2009) Detection of hepatitis B virus (HBV) DNA at femtomolar concentrations using a silica nanoparticle-enhanced microcantilever sensor. *Biosens Bioelectron* 25(1):130–135
63. Hassen WM, Chaix C, Abdelghani A, Bessueille F, Leonard D, Jaffrezic-Renault N (2008) An impedimetric DNA sensor based on functionalized magnetic nanoparticles for HIV and HBV detection. *Sens Actuators B* 134(2):755–760
64. Chang C-C, Chen C-C, Wei S-C, Lu H-H, Liang Y-H, Lin C-W (2012) Diagnostic devices for isothermal nucleic acid amplification. *Sensors* 12(6):8319–8337
65. Yao C, Xiang Y, Deng K, Xia H, Fu W (2013) Sensitive and specific HBV genomic DNA detection using RCA-based QCM biosensor. *Sens Actuators B* 181:382–387
66. Niemi A, Ferguson TM, Boyle DS (2011) Point-of-care nucleic acid testing for infectious diseases. *Trends Biotechnol* 29(5):240–250. doi:10.1016/j.tibtech.2011.01.007
67. Zhang DY, Brandwein M, Hsuih TC, Li H (1998) Amplification of target-specific, ligation-dependent circular probe. *Gene* 211(2):277–285
68. Hatch A, Sano T, Misasi J, Smith CL (1999) Rolling circle amplification of DNA immobilized on solid surfaces and its application to multiplex mutation detection. *Genet Anal* 15(2):35–40
69. McCarthy EL, Bickerstaff LE, da Cunha MP, Millard PJ (2007) Nucleic acid sensing by regenerable surface-associated isothermal rolling circle amplification. *Biosens Bioelectron* 22(7):1236–1244. doi:10.1016/j.bios.2006.05.001
70. Lee HY, Jeong H, Jung IY, Jang B, Seo YC, Lee H, Lee H (2015) DhITACT: DNA hydrogel formation by isothermal amplification of complementary target in fluidic channels. *Adv Mater* 27(23):3513–3517. doi:10.1002/adma.201500414
71. Mokhtarzadeh A, Dolatabadi JE, Abnous K, de la Guardia M, Ramezani M (2015) Nanomaterial-based cocaine aptasensors. *Biosens Bioelectron* 68:95–106. doi:10.1016/j.bios.2014.12.052
72. Wen Y, Pei H, Wan Y, Su Y, Huang Q, Song S, Fan C (2011) DNA nanostructure-decorated surfaces for enhanced aptamer-target binding and electrochemical cocaine sensors. *Anal Chem* 83(19):7418–7423. doi:10.1021/ac201491p
73. Zhang CY, Yeh HC, Kuroki MT, Wang TH (2005) Single-quantum-dot-based DNA nanosensor. *Nat Mater* 4(11):826–831
74. Gill R, Zayats M, Willner I (2008) Semiconductor quantum dots for bioanalysis. *Angew Chem* 47(40):7602–7625. doi:10.1002/anie.200800169
75. Li Y, Ji X, Liu B (2011) Chemiluminescence aptasensor for cocaine based on double-functionalized gold nanoprobe and functionalized magnetic microbeads. *Anal Bioanal Chem* 401(1):213–219. doi:10.1007/s00216-011-5064-6
76. Bi S, Yan Y, Yang X, Zhang S (2009) Gold nanolabels for new enhanced chemiluminescence immunoassay of alpha-fetoprotein based on magnetic beads. *Chemistry* 15(18):4704–4709. doi:10.1002/chem.200801722
77. Park SJ, Taton TA, Mirkin CA (2002) Array-based electrical detection of DNA with nanoparticle probes. *Science* 295(5559):1503–1506. doi:10.1126/science.1067003
78. He JL, Wu ZS, Zhou H, Wang HQ, Jiang JH, Shen GL, Yu RQ (2010) Fluorescence aptameric sensor for strand displacement amplification detection of cocaine. *Anal Chem* 82(4):1358–1364. doi:10.1021/ac902416u
79. Yang L, Fung CW, Cho EJ, Ellington AD (2007) Real-time rolling circle amplification for protein detection. *Anal Chem* 79(9):3320–3329. doi:10.1021/ac062186b
80. Espy MJ, Uhl JR, Sloan LM, Buckwalter SP, Jones MF, Vetter EA, Yao JD, Wengenack NL, Rosenblatt JE, Cockerill FR 3rd, Smith TF (2006) Real-time PCR in clinical microbiology: applications for routine laboratory testing. *Clin Microbiol Rev* 19(1):165–256. doi:10.1128/CMR.19.1.165-256.2006
81. Soderberg O, Gullberg M, Jarvius M, Ridderstrale K, Leuchowius KJ, Jarvius J, Wester K, Hydbring P, Bahram F, Larsson LG, Landegren U (2006) Direct observation of individual endogenous protein complexes in situ by proximity ligation. *Nat Methods* 3(12):995–1000. doi:10.1038/nmeth947
82. Nallur G, Luo C, Fang L, Cooley S, Dave V, Lambert J, Kukanskis K, Kingsmore S, Lasken R, Schweitzer B (2001) Signal amplification by rolling circle amplification on DNA microarrays. *Nucleic Acids Res* 29(23):e118
83. Di Giusto DA, Wlassoff WA, Gooding JJ, Messerle BA, King GC (2005) Proximity extension of circular DNA aptamers with real-time protein detection. *Nucleic Acids Res* 33(6):e64. doi:10.1093/nar/gni063
84. Kjallman TH, Peng H, Soeller C, Travas-Sejdic J (2008) Effect of probe density and hybridization temperature on the response of an electrochemical hairpin-DNA sensor. *Anal Chem* 80(24):9460–9466. doi:10.1021/ac801567d

85. Zhao XH, Kong RM, Zhang XB, Meng HM, Liu WN, Tan W, Shen GL, Yu RQ (2011) Graphene-DNAzyme based biosensor for amplified fluorescence "turn-on" detection of Pb^{2+} with a high selectivity. *Anal Chem* 83(13):5062–5066. doi:10.1021/ac200843x
86. Yin BC, Ye BC, Tan W, Wang H, Xie CC (2009) An allosteric dual-DNAzyme unimolecular probe for colorimetric detection of copper(II). *J Am Chem Soc* 131(41):14624–14625. doi:10.1021/ja9062426
87. Guo L, Nie D, Qiu C, Zheng Q, Wu H, Ye P, Hao Y, Fu F, Chen G (2012) A G-quadruplex based label-free fluorescent biosensor for lead ion. *Biosens Bioelectron* 35(1):123–127. doi:10.1016/j.bios.2012.02.031
88. He HZ, Leung KH, Yang H, Chan DS, Leung CH, Zhou J, Bourdoncle A, Mergny JL, Ma DL (2013) Label-free detection of sub-nanomolar lead(II) ions in aqueous solution using a metal-based luminescent switch-on probe. *Biosens Bioelectron* 41:871–874. doi:10.1016/j.bios.2012.08.060
89. Wen Y, Peng C, Li D, Zhuo L, He S, Wang L, Huang Q, Xu QH, Fan C (2011) Metal ion-modulated graphene-DNAzyme interactions: design of a nanoprobe for fluorescent detection of lead(II) ions with high sensitivity, selectivity and tunable dynamic range. *Chem Commun* 47(22):6278–6280. doi:10.1039/c1cc11486g
90. Zhu Y, Zeng GM, Zhang Y, Tang L, Chen J, Cheng M, Zhang LH, He L, Guo Y, He XX, Lai MY, He YB (2014) Highly sensitive electrochemical sensor using a MWCNTs/GNPs-modified electrode for lead(II) detection based on Pb^{2+} -induced G-rich DNA conformation. *Analyst, U K* 139(19):5014–5020. doi:10.1039/c4an00874j
91. Long YT, Kong C, Li DW, Li Y, Chowdhury S, Tian H (2011) Ultrasensitive determination of cysteine based on the photocurrent of Nafion-functionalized CdS-MV quantum dots on an ITO electrode. *Small* 7(12):1624–1628. doi:10.1002/smll.201100427
92. Lu W, Jin Y, Wang G, Chen D, Li J (2008) Enhanced photoelectrochemical method for linear DNA hybridization detection using Au-nanoparticle labeled DNA as probe onto titanium dioxide electrode. *Biosens Bioelectron* 23(10):1534–1539. doi:10.1016/j.bios.2008.01.011
93. Chen D, Zhang H, Li X, Li J (2010) Biofunctional titania nanotubes for visible-light-activated photoelectrochemical biosensing. *Anal Chem* 82(6):2253–2261. doi:10.1021/ac9021055
94. Zang Y, Lei J, Hao Q, Ju H (2014) "Signal-on" photoelectrochemical sensing strategy based on target-dependent aptamer conformational conversion for selective detection of lead(II) ion. *ACS Appl Mater Interfaces* 6(18):15991–15997. doi:10.1021/am503804g
95. Fan X, White IM (2011) Optofluidic microsystems for chemical and biological analysis. *Nat Photonics* 5(10):591–597. doi:10.1038/nphoton.2011.206
96. Long F, Zhu A, Wang H (2014) Optofluidics-based DNA structure-competitive aptasensor for rapid on-site detection of lead(II) in an aquatic environment. *Anal Chim Acta* 849:43–49. doi:10.1016/j.aca.2014.08.015
97. Yuan M, Li Y, Li J, Li C, Liu X, Lv J, Xu J, Liu H, Wang S, Zhu D (2007) A colorimetric and fluorometric dual-model assay for mercury ion by a molecule. *Org Lett* 9(12):2313–2316. doi:10.1021/ol0706399
98. Ye BC, Yin BC (2008) Highly sensitive detection of mercury(II) ions by fluorescence polarization enhanced by gold nanoparticles. *Angew Chem* 47(44):8386–8389. doi:10.1002/anie.200803069
99. Baby TT, Ramaprabhu S (2010) SiO_2 coated Fe_3O_4 magnetic nanoparticle dispersed multiwalled carbon nanotubes based amperometric glucose biosensor. *Talanta* 80(5):2016–2022. doi:10.1016/j.talanta.2009.11.010
100. Lakowicz JR (2006) Principles of fluorescence spectroscopy, 3rd edn. Springer, New York
101. Shen T, Yue Q, Jiang X, Wang L, Xu S, Li H, Gu X, Zhang S, Liu J (2013) A reusable and sensitive biosensor for total mercury in canned fish based on fluorescence polarization. *Talanta* 117:81–86. doi:10.1016/j.talanta.2013.08.017
102. Osman O, Zanini LF, Frenea-Robin M, Dumas-Bouchiat F, Dempsey NM, Reyne G, Buret F, Haddour N (2012) Monitoring the endocytosis of magnetic nanoparticles by cells using permanent micro-flux sources. *Biomed Microdevices* 14(5):947–954. doi:10.1007/s10544-012-9673-4
103. Upadhyay AK, Ting TW, Chen SM (2009) Amperometric biosensor for hydrogen peroxide based on coimmobilized horseradish peroxidase and methylene green in ormosils matrix with multiwalled carbon nanotubes. *Talanta* 79(1):38–45. doi:10.1016/j.talanta.2009.03.010
104. Li D, Wieckowska A, Willner I (2008) Optical analysis of Hg^{2+} ions by oligonucleotide-gold-nanoparticle hybrids and DNA-based machines. *Angew Chem* 47(21):3927–3931. doi:10.1002/anie.200705991
105. Liu J, Lu Y (2007) Rational design of "turn-on" allosteric DNAzyme catalytic beacons for aqueous mercury ions with ultra-high sensitivity and selectivity. *Angew Chem* 46(40):7587–7590. doi:10.1002/anie.200702006
106. Lee J, Jun H, Kim J (2009) Polydiacetylene-liposome microarrays for selective and sensitive mercury(II) detection. *Adv Mater* 21(36):3674–3677. doi:10.1002/adma.200900639
107. Yang YK, Ko SK, Shin I, Tae J (2007) Synthesis of a highly metal-selective rhodamine-based probe and its use for the in vivo monitoring of mercury. *Nat Protoc* 2(7):1740–1745. doi:10.1038/nprot.2007.246
108. Wang S, Forzani ES, Tao N (2007) Detection of heavy metal ions in water by high-resolution surface plasmon resonance spectroscopy combined with anodic stripping voltammetry. *Anal Chem* 79(12):4427–4432. doi:10.1021/ac0621773
109. Alvarez-Puebla RA, Liz-Marzan LM (2012) SERS detection of small inorganic molecules and ions. *Angew Chem* 51(45):11214–11223. doi:10.1002/anie.201204438
110. Zhang L, Chang H, Hirata A, Wu H, Xue QK, Chen M (2013) Nanoporous gold based optical sensor for sub-ppt detection of mercury ions. *ACS Nano* 7(5):4595–4600. doi:10.1021/nm4013737
111. Liu SJ, Nie HG, Jiang JH, Shen GL, Yu RQ (2009) Electrochemical sensor for mercury(II) based on conformational switch mediated by interstrand cooperative coordination. *Anal Chem* 81(14):5724–5730. doi:10.1021/ac900527f
112. Ramezani M, Mohammad Danesh N, Lavaee P, Abnous K, Mohammad Taghdisi S (2015) A novel colorimetric triple-helix molecular switch aptasensor for ultrasensitive detection of tetracycline. *Biosens Bioelectron* 70:181–187. doi:10.1016/j.bios.2015.03.040
113. Verdian-Doghaei A, Housaindokht MR, Abnous K (2014) A fluorescent aptasensor for potassium ion detection-based triple-helix molecular switch. *Anal Biochem* 466:72–75. doi:10.1016/j.ab.2014.08.014
114. Zheng J, Li JS, Jiang Y, Jin JY, Wang KM, Yang RH, Tan WH (2011) Design of aptamer-based sensing platform using triple-helix molecular switch. *Anal Chem* 83(17):6586–6592. doi:10.1021/AC201314y
115. Shariati S, Yamini Y, Esrafil A (2009) Carrier mediated hollow fiber liquid phase microextraction combined with HPLC-UV for preconcentration and determination of some tetracycline antibiotics. *J Chromatogr B* 877(4):393–400. doi:10.1016/j.jchromb.2008.12.042
116. Kurittu J, Lonnberg S, Virta M, Karp M (2000) A group-specific microbiological test for the detection of tetracycline residues in raw milk. *J Agric Food Chem* 48(8):3372–3377

117. Jeon M, Rhee Paeng I (2008) Quantitative detection of tetracycline residues in honey by a simple sensitive immunoassay. *Anal Chim Acta* 626(2):180–185. doi:10.1016/j.aca.2008.08.003
118. Zhou L, Li DJ, Gai L, Wang JP, Li YB (2012) Electrochemical aptasensor for the detection of tetracycline with multi-walled carbon nanotubes amplification. *Sens Actuators B* 162(1):201–208. doi:10.1016/j.snb.2011.12.067
119. Tao HL, Wei LL, Liang AH, Li JF, Jiang ZL, Jiang HS (2010) Highly sensitive resonance scattering detection of DNA hybridization using aptamer-modified gold nanoparticle as catalyst. *Plasmonics* 5(2):189–198. doi:10.1007/s11468-010-9133-z
120. Luo Y, He L, Zhan S, Wu Y, Liu L, Zhi W, Zhou P (2014) Ultrasensitive resonance scattering (RS) spectral detection for trace tetracycline in milk using aptamer-coated nanogold (ACNG) as a catalyst. *J Agric Food Chem* 62(5):1032–1037. doi:10.1021/jf403566e
121. Battig MR, Soontornworajit B, Wang Y (2012) Programmable release of multiple protein drugs from aptamer-functionalized hydrogels via nucleic acid hybridization. *J Am Chem Soc* 134(30):12410–12413. doi:10.1021/ja305238a
122. Wu Y, Li C, Boldt F, Wang Y, Kuan SL, Tran TT, Mikhalevich V, Fortsch C, Barth H, Yang Z, Liu D, Weil T (2014) Programmable protein-DNA hybrid hydrogels for the immobilization and release of functional proteins. *Chem Commun* 50(93):14620–14622. doi:10.1039/c4cc07144a
123. Liu R, Huang Y, Ma Y, Jia S, Gao M, Li J, Zhang H, Xu D, Wu M, Chen Y, Zhu Z, Yang C (2015) Design and synthesis of target-responsive aptamer-cross-linked hydrogel for visual quantitative detection of ochratoxin A. *ACS Appl Mater Interfaces* 7(12):6982–6990. doi:10.1021/acsami.5b01120
124. Song Y, Zhang Y, Bernard PE, Reuben JM, Ueno NT, Arlinghaus RB, Zu Y, Qin L (2012) Multiplexed volumetric bar-chart chip for point-of-care diagnostics. *Nat Commun* 3:1283. doi:10.1038/ncomms2292
125. Park JH, Byun JY, Mun H, Shim WB, Shin YB, Li T, Kim MG (2014) A regeneratable, label-free, localized surface plasmon resonance (LSPR) aptasensor for the detection of ochratoxin A. *Biosens Bioelectron* 59:321–327. doi:10.1016/j.bios.2014.03.059
126. Cho EM, Lee HS, Eom CY, Ohta A (2010) Construction of high sensitive detection system for endocrine disruptors with yeast n-alkane-assimilating *Yarrowia lipolytica*. *J Microbiol Biotechnol* 20(11):1563–1570
127. Alonso-Magdalena P, Quesada I, Nadal A (2011) Endocrine disruptors in the etiology of type 2 diabetes mellitus. *Nat Rev Endocrinol* 7(6):346–353. doi:10.1038/nrendo.2011.56
128. Lehmann GM, Christensen K, Maddaloni M, Phillips LJ (2015) Evaluating health risks from inhaled polychlorinated biphenyls: research needs for addressing uncertainty. *Environ Health Perspect* 123(2):109–113. doi:10.1289/ehp.1408564
129. Rezg R, El-Fazaa S, Gharbi N, Mornagui B (2014) Bisphenol A and human chronic diseases: current evidences, possible mechanisms, and future perspectives. *Environ Int* 64:83–90. doi:10.1016/j.envint.2013.12.007